https://doi.org/10.5194/acp-2020-101
Preprint. Discussion started: 17 February 2020

Atmospheric Chemistry and Physics Discussions

Study of the dependence of stratospheric ozone long-term trends on local solar time

Eliane Maillard Barras[1], Alexander Haefele[1], Liliane Nguyen[2], Fiona Tummon[1], William T. Ball[3,4], Eugene V. Rozanov[4], Rolf Rüfenacht[1], Klemens Hocke[5], Leonie Bernet[5], Niklaus Kämpfer[5], Gerald Nedoluha[6], and Ian Boyd[7]

[1]Federal Office of Meteorology and Climatology, MeteoSwiss, Switzerland
[2]ISE, Institute for Environmental Sciences, University of Geneva, Switzerland
[3]Institute for Atmospheric and Climate Science, Swiss Federal Institute of Technology Zurich, Switzerland
[4]Physikalisch-Meteorologisches Observatorium Davos World Radiation Centre, Switzerland
[5]Institute of Applied Physics and Oeschger Centre for Climate Change Research, University of Bern, Bern, Switzerland
[6]Naval Research Laboratory, Washington DC, USA
[7]BC Scientific Consulting LLC, New Zealand

Correspondence: Eliane Maillard Barras (eliane.maillard@meteoswiss.ch)

Abstract. Multi-instrument comparison analyses are essential to assess the long-term stability of data records by estimating the drift and bias of instruments. The ozone profile dataset from the SOMORA microwave radiometer (MWR) in Payerne, Switzerland, was compared with profiles from the GROMOS MWR in Bern, Switzerland, satellite instruments (MLS, MIPAS, HALOE, SCHIAMACHY, GOMOS), and profiles simulated by the SOCOL v3.0 chemistry-climate model (CCM). The Payerne MWR dataset has been homogenized ~~to ensure a stable measurement contribution to the ozone profiles and~~ to take into account the effects of three major instrument upgrades. At pressure levels smaller than 0.59 hPa (above ~50 km), the homogenization corrections to be applied to the Payerne MWR ozone profiles are dependent on local solar time (LST). Due to the lack of reference measurements with a comparable measurement contribution at a high time resolution, a comprehensive homogenization of the sub-daily ozone profiles was possible only for pressure levels larger than 0.59 hPa.

The long-term stability and mean biases of the time series were estimated as a function of the measurement time (day- and nighttime). The homogenized Payerne MWR ozone data agrees within ±5% with the MLS dataset over the 30 to 65 km altitude range and within ±10% of HARMOZ datasets over the 30 to 65 km altitude range. In the upper stratosphere, there is a large nighttime difference between Payerne MWR and other datasets, which is likely a result of the mesospheric signal aliasing with lower levels in the stratosphere due to a lower vertical resolution at that altitude. Hence, the induced bias at 55 km is considered an instrumental artefact and is not further analyzed ~~and discussed~~.

In the upper stratosphere (5–1 hPa, 35–48 km), the Payerne MWR trends are significantly positive at 2 to 3 %/decade. This is in accordance with the northern hemisphere (NH) trends reported by other ground-based instruments in the SPARC LOTUS project. The reason for variability in the reported long-term ground-based and satellite ozone profile trends has multiple possibilities. To determine what part of the variability comes from measurement timing, MWR trends were estimated for each hour of the day with a multiple linear regression model to quantify trends as a function of LST. In the mid- and upper stratosphere, differences as a function of LST are reported for both the MWR and simulated trends for the 2000-2016 period.

https://doi.org/10.5194/acp-2020-101
Preprint. Discussion started: 17 February 2020

Atmospheric Chemistry and Physics Discussions

However, these differences are not significant at the 95% confidence level. In the lower mesosphere (1–0.1 hPa, 48–65 km), the 2010-2018 day- and nighttime trends have been considered. Here again, the variation of the trend with LST is not significant at the 95% confidence level. Based on these results we conclude that trend differences between instruments cannot to be attributed to a systematic temporal sampling. effect

1 Introduction

the

Since the discovery of the ozone hole over Antarctica in 1985 (Chubachi, 1985; Farman et al., 1985), understanding the mechanisms that drive stratospheric ozone trends has been a major area of interest in atmospheric research. After the first insights into the impacts of the Montreal Protocol on stratospheric ozone variability (Mäder et al., 2010, and references therein), the challenge is now to confirm the efficacy of the Montreal protocol by assessing stratospheric ozone recovery. Moreover, as ozone recovery is strongly influenced by climate change (Eyring et al., 2010; Meul et al., 2016), the continued monitoring of stratospheric ozone and its vertical structure is essential.

Chemical processes involved in polar ozone depletion also affect ozone in the stratosphere at a global scale (Solomon, 1999).

Besides the Chapman cycle

The main chemical species involved in stratospheric ozone loss processes are chlorine compounds (HCl, ClOx), hydroxyl radicals (OH), and nitrogen oxides (NO_x), while stratospheric temperature (T) influences the rate of both ozone production and destruction. The effect of chlorine compounds on ozone loss has been extensively described in the literature (Farman et al., 1985; Solomon, 1999) since its first mention by Molina and S. (1974). In the stratosphere, the variability of NO_x plays a key role in the variability of ozone (Hendrick et al., 2012; Nedoluha et al., 2015a; Wang et al., 2014; E. et al., 2019). The NO_x catalytic cycle counteracts the accumulation of ozone during the day and leads to a negative correlation between anomalies in NO_x and the amplitude of the ozone diurnal cycle (Schanz et al., 2014). Finally, the negative correlation of ozone and temperature is mainly due to the temperature dependence of the rate coefficients of the Chapman cycle reactions (Barnett et al., 1975; Craig and Ohring, 1958).

Please specify what kind of variability you mean (in time, in space, what scales)

In the mesosphere, OH radicals destroy ozone in auto-catalytic cycles and dominate the ozone budget above about 1 hPa (Lossow et al., 2019). Mesospheric OH is predominantly produced by the photo-dissociation of water vapor and OH_x measurements can be used as a proxy for mesospheric H_2O (Newnham et al., 2019). The interaction of ozone with mesospheric water vapor is further described in Flury et al. (2009), Haefele et al. (2008), and references therein.

In the northern hemisphere (NH), upper stratospheric ozone is reported to be increasing by 2-3% per decade, due to both declining levels of ozone depleting substances and stratospheric cooling. These estimates are based on measurements from satellites and ground-based instruments as well as chemistry-climate models simulations (Petropavlovskikh et al., 2019). This recovery is statistically significant down to 4 hPa (∼38 km), however, at altitudes below this level, NH mid-latitude trends are not statistically significant. For the lowermost stratosphere, they even vary considerably between datasets (Bernet et al., 2019) although there is evidence for ongoing negative trends in some NH regions (Ball et al., 2018, 2019). For the mesosphere, negative trends have been reported in Moreira et al. (2015) and Kyrölä et al. (2013). In the southern hemisphere (SH) mid-latitudes, satellites and ground-based datasets show statistically insignificant negative trends in the middle and lower stratosphere while

https://doi.org/10.5194/acp-2020-101
Preprint. Discussion started: 17 February 2020

Atmospheric Chemistry and Physics Discussions

upper stratospheric trends are significantly positive at 2% per decade mainly close to 2 hPa (Petropavlovskikh et al., 2019). In the tropics, a continuous decline in the middle and lower stratosphere is simulated by chemistry-climate models and negative trends are retrieved from satellite- and ground-based measurements (Petropavlovskikh et al., 2019) which significance and magnitude are datasets dependent. The persistent negative trends are likely a consequence of radiative and dynamical forcing from climate change (Chipperfield et al., 2017). In the tropical upper stratosphere trends are also positive, even if smaller than those in the mid-latitudes. what is first? what exactly do you mean? I would say, that in contrast to the other pa

Few studies report lower mesospheric (altitudes above 0.6 hPa) ozone trends based on measurements for the period after 1998. Moreira et al. (2015) report negative trends up to -4% per decade for the 1997-2015 period between 52 and 67 km in the NH. In Marsh et al. (2003), negative mesospheric long-term trends of -4% per year are derived from HALOE sunset (SS) measurements before 2003.

Discrepancies between the post-1998 ozone profile trends calculated from ground-based instruments, satellite datasets and chemistry-climate models and the large uncertainties on the trends show that it is difficult to clearly provide evidence of stratospheric ozone recovery (Steinbrecht et al., 2017; Ball et al., 2017; Petropavlovskikh et al., 2019). Besides information on the stability and drift of the measurements (Hubert et al., 2016), consideration of the ozone diurnal variability (Studer et al., 2014) and of the spatial and temporal sampling of the dataset (Damadeo et al., 2018) is of primary importance to understanding differences in the trends and to reduce the uncertainty associated with them. The variation of the trends with LST has to be quantified to calculate representative trends derived from sun-synchronous satellite measurements and ensure a proper comparison of these trends with those estimated from ground-based instruments, or to ensure a proper comparison of trends estimated from instruments with different measurement schedules. The consistent high time resolution of ground-based MWR instruments make them ideal for excluding (analysing) this sampling bias from the parameters influencing trend estimates.

In this study, we first carefully homogenize the SOMORA Payerne MWR ozone profile dataset and validate this dataset against simultaneous ozone profiles measured by satellites. We then investigate the effect of the ozone diurnal cycle on the post-2000 (after the year 2000) linear trend by calculating long-term trends for each hour of the day and night with a multiple linear regression (MLR) model. Finally we compare the SOMORA Payerne MWR ozone trends in the upper and middle stratosphere to trends of OH, NO_x and T derived from the SOCOL v3.0 CCM, to investigate the correlations between the long-term variability of ozone, water vapor, nitrous oxide, and temperature, particularly at the diurnal scale.

The paper is organized as follows: Section 2 describes the ozone datasets measured by individual instruments. Section 3 is dedicated to the description of the methods used to calculate the diurnal cycle and trends. In Sect. 4, we describe and discuss the results of the SOMORA Payerne MWR validation and of the dependence of the MLR trends as a function of the time of day. Conclusions about the variability of the long-term stratospheric ozone trends are provided in Sect. 5.

https://doi.org/10.5194/acp-2020-101
Preprint. Discussion started: 17 February 2020


Atmospheric Chemistry and Physics Discussions

2 Data Sources

2.1 Stratospheric Ozone MOnitoring RAdiometer (SOMORA)

The microwave radiometer SOMORA, hereafter referred to as the Payerne MWR, is located in Payerne (46.82° N, 6.95° E, 491 m), Switzerland, and has been operated continuously by MeteoSwiss since January 2000. Ozone profile retrievals are obtained independent of weather conditions throughout the diurnal cycle, forming a dataset with a constant and stable time sampling over two decades. Ozone profiles are provided in volume mixing ratio (ppmv) on a pressure grid between 47.3 and 0.05 hPa. The vertical resolution is 8–10 km from 47 to 1.8 hPa (20 to 40 km), increasing to 15–20 km at 0.18 hPa (60 km) (Maillard Barras et al., 2015). The measurement contribution is above 80% from 47 to 0.27 hPa (20 to 57 km). The Payerne MWR is included in the Network for the Detection of Atmospheric Composition Change (NDACC).

2.1.1 Measurement principles and profile retrieval

Developed in 2000 by the University of Bern (Calisesi, 2000), the Payerne MWR is a total power microwave radiometer measuring the thermal emission line of ozone at 142.175 GHz. The electromagnetic radiation is measured at an antenna elevation angle of 39° and the brightness temperatures range from 80 to 260 K. The Payerne MWR is calibrated using a hot load heated and stabilized at 300 K and a cold load at 77 K cooled with liquid nitrogen. A rotating planar mirror is used as a switch between the radiation sources. A Martin-Puplett interferometer (sideband filter) picks out the frequency band around 142 GHz. Outgoing from the front-end part (quasi optics), the signal is amplified and down-converted in frequency to 7.1 GHz (mixer) by means of a constant-frequency signal (GUNN oscillator). The signal is further down-converted in two steps (intermediate step at 1.5GHz/1GHz) to the baseband (0-1 GHz). The spectral distribution, i.e. voltage as a function of channel or frequency, is measured by Acousto-optical spectrometers (AOS) in the first decade and since then by an Acquiris Fast-Fourier-Transform spectrometer (FFTS) with 16384 channels distributed over 1GHz bandwidth.

The pressure broadening effect on the line allows the retrieval of the vertical ozone profile from the measured spectrum using an a priori profile, a radiative transfer simulation (forward model, ARTS (Buehler et al., 2005)), and the optimal estimation method (OEM, Qpack (Eriksson et al., 2005)) based on Rodgers (2000).

The required a priori information is taken from a monthly-varying climatology (called the ML climatology and described in McPeters and Labow (2012) formed by combining data from Aura MLS (2004-2010) with data from balloon radiosondes (1988-2010)). Ozone below 8 km is based on sonde measurements, from 16 km to 65 km it is based on MLS measurements, and above 65 km a climatological standard profile combining 5 satellite ozone datasets is used (described in Keating et al. (1990)). Radiosonde and MLS data are blended in the tropospheric transition region. The ML climatology is combined with the Keating standard profile reference in the mesospheric transition region.

The diagonal elements of the a priori covariance matrix are given by the variance of the ML climatology. The off-diagonal elements are parameterized with an exponentially decaying correlation function using a correlation length of 3 km. The di-

https://doi.org/10.5194/acp-2020-101
Preprint. Discussion started: 17 February 2020


Atmospheric Chemistry and Physics Discussions

agonal elements of the error covariance matrix of the measured spectrum are estimated from the variance of the wings of the measured spectrum. The off-diagonal elements of the measurement error covariance matrix are zero.

The retrieval is characterized by the averaging kernel (AVK) matrix describing the changes in the retrieved profile as a function of changes in the true profile. The width of the AVKs is a measure of the vertical resolution of the retrievals and the area of the AVKs indicates the measurement contribution to the retrieved profile (Rodgers, 2000). The ozone profile is considered as reliable when the measurement contribution (MC) dominates the a priori information, i.e. when the measurement contribution is higher than 80%. Figure 1 shows the Payerne MWR AVKs and the MC ($\times 0.5$) for one sample month (January 2013). As a non-specialist for MWR observations, I wonder how th

2.1.2 Data quality and reliability

The total uncertainty is calculated for each retrieved profile accounting for the following sources of uncertainty: measurement noise, tropospheric attenuation, calibration load temperatures, spectroscopy, atmospheric temperature profile, and smoothing. The dominant source of uncertainty is smoothing because of the instrument's limited vertical resolution and is on the order of 15-20% of the ozone content. The second most important contribution is the measurement noise on the spectra amounting to 3-7% error when using a standard integration time of 1 hour. Tropospheric attenuation correction, the pressure-broadening coefficient of the observed line, calibration loads temperatures, and the atmospheric temperature profile (Payerne radiosondes combined with the ECMWF ERA-interim data) amount to an uncertainty of less than 3%.

2.1.3 Homogenization

2.1.3.1 Homogenization of the Payerne MWR AOS and FFTS time series

Spectral analysis of the Payerne MWR measurements was performed using two acousto-optical spectrometers (AOS) from January 2000 to October 2010; the AOS had a total bandwidth of 1 GHz, with a frequency resolution varying from 24 kHz at the line center to 980 kHz at the wings. In September 2009, an Acquiris fast Fourier transform spectrometer (FFTS) was added as a back end to the Payerne MWR. The FFTS covers a total bandwidth of 1GHz with 16384 channels, providing a frequency resolution of 61 kHz. This technical upgrade introduced a discontinuity in the timeseries, requiring an homogenization of the dataset. The AOS and FFTS were used in parallel for one year to ensure a proper homogenization of the transition.

The measurement contributions to simultaneous ozone profiles retrieved from the AOS and FFTS measurements were compared for the overlap period of one year. In Fig. 2 the monthly means of the measurement contribution at 0.4 hPa as a % of the ozone profile are plotted against the monthly means of the diurnal cycle amplitude (maximum-to-minimum difference) as a % of the midnight ozone value for the 2000-2016 measurement period. A clear negative correlation between the amplitude of the ozone diurnal cycle and the measurement contribution is shown for the lower mesosphere. A low measurement contribution means there is a large a priori contribution. Since the a priori profile is a standard climatological ozone profile without any diurnal variation, the lower the measurement contribution, the lower the diurnal cycle amplitude. Since the ozone diurnal cycle amplitude is correlated to the measurement contribution value, a proper homogenization should not be limited to a correction

I would have expected you show differences for that year. Please motivate what you are doing.

https://doi.org/10.5194/acp-2020-101
Preprint. Discussion started: 17 February 2020

Atmospheric Chemistry and Physics Discussions

of the bias between profiles retrieved from the spectra measured by the 2 spectral setups but should include a full homogenization of the characteristics of the retrieval (measurement response and vertical resolution). The AOS and FFTS ozone profile datasets used in this study were harmonized by ensuring a constant measurement contribution to the retrieved ozone profiles between 47 and 0.05 hPa (20 and 70km). The integration time for one ozone profile therefore varies from 30 min to 2 h. For a stable measurement contribution over the AOS to FFTS transition in the upper stratosphere/lower mesosphere, FFTS measurements require being accumulated over 2 h (FFTS2h dataset). However, in the altitude range where the measurement contribution is much larger than 80%, a FFTS signal accumulation time of 1 h is sufficient, therefore allowing a higher time resolution dataset (FFTS1h dataset). The FFTS1h data are used for the middle stratosphere and upper stratosphere below 48km where high time resolution without any degradation of the measurement contribution is required. The FFTS2h data are used for the lower mesosphere where the consistency of the measurement contribution is more important than the time resolution requirement.

what do you mean with constant? In time? or between altitude range?

what about the AOS?

The bias between the profiles retrieved from the two spectral measurement setups was then determined from simultaneous measurements during the one year transition period. The mean absolute difference for each profile layer was subtracted from the AOS profiles, keeping the FFTS profile dataset unchanged. Bias values are within 10% between 47 and 0.05 hPa (20 to 70km).

The application range of the correction offset depends to a large extent on the way the offset is calculated. The AOS to FFTS correction offset, when determined by the comparison of simultaneous monthly means, should be applied only to the global monthly means time series and not to sub-daily monthly means. To homogenise the AOS to FFTS datasets for both the 1h and 2h bins, the AOS to FFTS correction offset variation with LST was determined. As shown in Fig. 3a and b, the correction offsets do not vary significantly with LST below 50 km (0.6 hPa). However, in the lower mesosphere, the AOS to FFTS 2h correction offset is lower during daytime than during nighttime, following the diurnal variation of ozone. A correction offset depending on the LST has to be applied to the AOS data above 50 km for a proper homogenization of time series when LST depending monthly means are considered.

Can you explain that behaviour?

2.1.3.2 Time series corrections for technical issues

Since January 2000 the Payerne MWR has been affected by several technical issues: the mixer diode was replaced in 2001, the front-end changed in 2005, and the GUNN oscillator repaired in 2009. Each of these major technical interventions could potentially affect the measured spectrum by modifying the baseline shape and the receiver temperature. The retrieval was adapted between the 2001 and 2005 interventions by considering a sinusoidal function in the spectrum background removal. For the correction of the effects from the 2005 and 2009 interventions, homogenization of the ozone profile time series was performed using coincident AVK convolved ozone profiles from the Bern MWR and AURA/MLS. The absolute mean differences of the deseasonalized coincident datasets were considered. For the 2005 homogenization, the difference between the Payerne MWR AOS dataset and the Bern MWR after the upgrade (in 2007, since in 2006 the Bern MWR dataset presents a negative anomaly compared to other instruments (Bernet et al., 2019)) was subtracted from the difference between the Payerne MWR AOS dataset and the Bern MWR before the upgrade (in 2004). This relative bias was then removed from the Payerne MWR profile

https://doi.org/10.5194/acp-2020-101
Preprint. Discussion started: 17 February 2020


Atmospheric Chemistry and Physics Discussions

dataset prior to the 2005 intervention. For the 2009 homogenization, the difference between the Payerne MWR AOS dataset and MLS in 2010 was subtracted from the difference between the Payerne MWR AOS dataset and MLS in 2008. This relative bias was then removed from the Payerne MWR profile dataset prior to the 2009 intervention. These homogenizations are only possible if it is assumed the reference instruments (i.e. the Bern MWR and MLS) do not drift during the periods considered. The Bern MWR dataset does not present any anomalies compared to other ground-based instruments in 2004 and 2007 (Bernet et al., 2019) and the MLS dataset does not present any anomalies compared to other satellite instruments between 2008 and 2010 (Hubert et al., 2016). Note that the mean drifts of 5-10%/decade measured between the MWRs and the satellites shown in (Hubert et al., 2016; Hubert, 2019) are not representative of the drifts during the two year periods considered here.

Here again, the 2005 and 2009 technical issues affect the ozone profiles above 50 km differently depending on the LST. Figure 3c and d show the correction offset variation with LST for the 2005 and 2009 upgrades. Correction offsets have to be evaluated by considering the time bins. While a correction for 2005 is possible using the Bern MWR high time resolution dataset (Fig. 3c), in 2009 the lack of coincident measurements at high time resolution makes any LST-resolved correction very difficult (impossible). Coincident MLS measurements are available only twice a day (1 am and 1 pm overpasses) and the Bern MWR underwent an upgrade in 2009, meaning the stability of the dataset in term of measurement contribution during this particular period is uncertain (Fig. 3d).

A homogenised version of the 2000-2018 Payerne MWR dataset was thus made available for monthly means without any LST distinction above 50 km. For this study, we used the homogenised 2000-2018 timeseries of 1h LST-resolved monthly means for altitudes below 50km, and the FFTS 2010-2018 timeseries of 2h LST-resolved monthly means for altitudes above 50km. In order to show the effect of homogenization, please sho

2.2 Other MWRs

2.2.1 GROMOS Bern microwave radiometer

The GROMOS (GROund-based Millimeter-wave Ozone Spectrometer) microwave radiometer, hereafter referred to as the Bern MWR, is a ground-based ozone microwave radiometer continuously observing the middle atmosphere above Bern (46.95° N, 7.44° E, 577 m), Switzerland, since November 1994. Like the Payerne MWR, the Bern MWR measures the thermal microwave emission of the rotational transition of ozone at 142.175 GHz, switching between the atmosphere, a cold load (liquid nitrogen at 80 K) and a hot load (electrical heater at 313 K). The Bern MWR spectral distribution has been measured since 1994 by a filter bank spectrometer with an integration time of 1h (frequency resolution of 100 MHz to 200 kHz) replaced in 2009 by an FFTS with an integration time of 30min (30.5 kHz frequency resolution). For technical details about the instrument, the measurement principle and the retrieval procedure, see Moreira et al. (2015) and Bernet et al. (2019, and references included therein). The vertical resolution is between 8–12 km in the stratosphere and increases with altitude to 20–25 km in the lower mesosphere. The measurement contribution is above 80% from 20 to 52 km Moreira et al. (2015). The Bern MWR also contributes to NDACC.

https://doi.org/10.5194/acp-2020-101
Preprint. Discussion started: 17 February 2020


Atmospheric Chemistry and Physics Discussions

2.2.2 Mauna Loa MWR

The Mauna Loa MWR (MLO MWR) operated by U.S. the Naval Research Laboratory measures the emission spectrum of the ozone line at 110.836 GHz. It has been in operation at Mauna Loa (19.54° N, 155.6° W, 3397 m), USA, since 1995 and also contributes to NDACC. The spectral intensities are calibrated with black body sources at ambient and liquid nitrogen temperatures. The experimental technique is described in Parrish et al. (1992), and technical details about the instrument are provided in Parrish (1994). While the basic radiometric features are similar to the Bern and Payerne MWRs, the MLO MWR receiver is cryogenically cooled and the spectral distribution is measured by a filter bank spectrometer. The ozone mixing ratio profiles are retrieved from the spectra using an adaptation of the optimal estimation method of Rodgers (Connor et al., 1995; Rodgers, 2000).

The vertical resolution is 6 km at an altitude of 32 km, between 6 and 8 km from 20 to 42 km, and then increases to 14 km at 65 km. The measurement contribution is above 80% from 20 to 70 km. While hourly measurements are performed for the purpose of diurnal cycle studies (Parrish et al., 2014), data are deposited in the NDACC with a 6-hourly time resolution. The NDACC dataset is used in this study. The MLO MWR underwent a major spectrometer upgrade between 2015 and 2017. For this study, only data until May 2015 have been used.

2.3 Satellites

The Payerne MWR is compared to the three instruments from the ENVISAT satellite: GOMOS (Global Ozone Monitoring by Occultation of Stars), MIPAS (Michelson Interferometer for Passive Atmospheric Sounding) and SCIAMACHY (SCanning Imaging Absorption spectroMeter for Atmospheric CHartographY), as well as to the MLS (Microwave Limb Sounder) on the Aura satellite and HALOE (Halogen Occultation Experiment) on the UARS satellite. The ENVISAT instruments are part of the Ozone Climate Change Initiative (Ozone CCI).

The HARMOZ dataset (Sofieva et al., 2013) is composed of ENVISAT ozone profiles in number density on a common pressure grid, which corresponds to a vertical sampling of 2–3 km. HARMOZ and HALOE data centered 10° by 10° around Payerne were selected (equivalent to an area of approximately 1110 km by 760 km). The collocation criterion for MLS satellite data is ±3° in latitude and ±5° in longitude (an area of approximately 666 km by 760km). This criterion ensures a sufficient number of collocated measurements and thus provides reliable bias estimates.

2.3.1 MLS

MLS is a microwave limb-sounding radiometer onboard the Aura Earth observing satellite. Ozone profiles are retrieved from MLS radiance measurements at 240 GHz. Details about the Aura mission can be found in Waters et al. (2006). In this study we use ozone profiles from the version 4.2 dataset (Livesey, 2018). MLS measures ozone profiles from 10 to 75 km with the vertical resolution ranging from to 2.5 to 4 km. MLS passes over Payerne at 1:30 UTC and 13:30 UTC. For the comparison with coincident Payerne MWR ozone profiles, the MLS profiles are convolved to the Payerne MWR vertical resolution using AVKs.

https://doi.org/10.5194/acp-2020-101
Preprint. Discussion started: 17 February 2020


Atmospheric Chemistry and Physics Discussions

2.3.2 ENVISAT

MIPAS is an infrared limb emission Fourier transform spectrometer (spectral range from 685 to 2410 cm^{-1}) on board the ENVISAT satellite. MIPAS provided profiles of H_2O, O_3, HNO_3, CH_4, N_2O and NO_2 from 2002 to 2012. Stratospheric ozone profiles are retrieved with the version V7R_O3_240 research processor developed at KIT IMK/IAA via constrained inverse modeling of limb radiances (Laeng et al., 2017). Data used in this study are the OR (Optimized Resolution) dataset from 2005 to 2012. MIPAS measured ozone profiles from 10-80 km, with a vertical resolution ranging from 2.4 km at an altitude of 10 km to 3.6 km at 30 km and 5 km at 70 km.

GOMOS was a stellar occultation instrument on board ENVISAT from 2002 to 2012 (Bertaux et al., 2010). GBL (Gomos Bright Light) measured the atmospheric limb radiance of scattered sunlight (Tukiainen et al., 2015). Ozone profiles are retrieved using the ESA IPF v6 processor (Sofieva et al., 2017) from the ultraviolet and visible spectrometer measurements at wavelengths between 250 and 692 nm with a two-step inversion (Kyrölä et al., 2010). ENVISAT overpass times for Payerne are 10:00 UTC (GBL dataset) and 22:00 UTC (GOMOS dataset). GOMOS measured ozone profiles from 20-100 km, with a vertical resolution of 2 km below altitudes of 30 km and 3 km above 40 km.

SCIAMACHY was a spaceborne spectrometer that measured the upwelling radiation from the Earth's atmosphere in the UV, visible, near-infrared and shortwave-infrared spectral ranges. A detailed description of the instrument and its measurement modes can be found in Bovensmann et al. (1999). Ozone profiles used in this study are retrieved using the UBR limb retrieval algorithm (V3_5). SCIAMACHY measured ozone profiles from 15-40 km, with a vertical resolution of 3 km. While measuring, SCIAMACHY passed over Payerne at 10:00 UTC. The MIPAS, GOMOS, GBL and SCIAMACHY profiles are AVK-convolved to the vertical resolution of the Payerne MWR and converted from number density (HARMOZ dataset) to ppm is carried out using ECMWF temperature profiles.

2.3.3 HALOE

HALOE was a mid-infrared solar occultation instrument on board the UARS (Upper Atmosphere Research Satellite) from 1991 to 2005 (Russell et al., 1993). HALOE retrieved vertical profiles of O_3, HCl, HF, CH_4, H_2O, NO, NO_2, aerosols and temperature from 15 daily sunrise (SR) and sunset (SS) measurements equally spaced in longitude. Data used in this study are the third public release record (v19). HALOE measured ozone profiles from 15 to 80 km with a vertical resolution of 3-5 km. For comparison with coincident Payerne MWR ozone profiles, the HALOE profiles are AVK-convolved to the Payerne MWR vertical resolution.

2.4 SOCOL CCM

The SOlar Climate Ozone Links (SOCOL) CCM consists of the middle atmosphere version of the MA-ECHAM general circulation model (Roeckner et al., 2003; Giorgetta et al., 2006), with 39 vertical levels between the surface and 0.01 hPa (∼80 km) coupled to the Model for Evaluation of oZONe trends (MEZON) chemistry module (Egorova et al., 2003).Dynamical and physical processes in the CCM SOCOL are calculated every 15 minutes within the model, while full radiative and chemical

https://doi.org/10.5194/acp-2020-101
Preprint. Discussion started: 17 February 2020


Atmospheric Chemistry and Physics Discussions

calculations are performed every two hours. Chemical constituents are transported using a flux-form semi-Lagrangian scheme (Lin and Rood, 1996). Original version includes 41 chemical species interacting participating in 140 gas-phase, 46 photolysis, and 16 heterogeneous reactions. The CCM SOCOL exploits T42 horizontal spectral truncation, which corresponds approximately to 2.5° by 2.5° resolution. The first model version was described and evaluated by Stenke et al. (2013). The model now includes an isoprene oxidation mechanism (Poeschl et al., 2000), the online calculation of lightning NOx emissions (Price and Rind, 1992), treatment of the effects produced by different energetic particles (Rozanov et al., 2012), updated reaction rates and absorption cross sections (Sander, 2011), improved solar heating rates (Sukhodolov et al., 2014), as well as a parameterization of cloud effects on photolysis rates(Chang et al., 1987). All considered halogenated ozone depleting species are transported as separate tracers.

The SOCOL v3.0 dataset has been validated in the troposphere and stratosphere with satellites, NDACC ground-based instruments and other CCMs (Staehelin et al., 2017; Revell et al., 2015; Stenke et al., 2013). Stratospheric ozone trends derived from SOCOL v3.0 in specified dynamics mode have also been compared with trends derived from measurements (Ball et al., 2018). For the comparison with ground-based observations the model outputs were horizontally interpolated to the location of Payerne from the adjacent grid cells. An AVK convolution was also applied to the model data for comparison with the Payerne MWR profiles.

3 Methods

3.1 Diurnal cycle calculation

The amplitude of the ozone diurnal cycle depends on altitude and varies seasonally. Above 0.59 hPa (50 km), the daytime ozone values are 15-25% lower compared to the nighttime values, while at 5 hPa (35 km) afternoon values are up to 3% larger compared to nighttime values. The ozone diurnal cycle in the mesosphere has been intensively studied (Pallister and Tuck, 1983; Ricaud et al., 1996; Vaughan, 1984). The diurnal cycle of ozone in the stratosphere has been reported in Haefele et al. (2008), and the interannual variations of the ozone diurnal cycle described in Studer et al. (2014).

The diurnal ozone cycle is calculated relative to the nighttime value by:

$$O_{3,rel} = \frac{O_3 - O_{3,midnight}}{O_{3,midnight}} \quad (1)$$

where $O_{3,midnight}$ is an average of the ozone values from 22:00 to 02:00 LST at each pressure level.

3.2 Trend calculation

Trend estimates are obtained by fitting a multi-linear regression (MLR) function to the monthly mean ozone time series from each dataset. Trends are calculated for each pressure level independently and form a trend profile. We calculate average daytime (10:00-14:00 LST) and nighttime (22:00-2:00 LST) trends as well as the trends for each hour of the day. The following MLR

https://doi.org/10.5194/acp-2020-101
Preprint. Discussion started: 17 February 2020


Atmospheric Chemistry and Physics Discussions

function is used:

$$O_3(t) = a + c_0\ t + \sum_{i=1}^{2} c_i \sin\left(\frac{2\pi i}{12} t\right) + \sum_{j=1}^{2} c_{j+2} \cos\left(\frac{2\pi j}{12} t\right) + c_5 \mathrm{SOL}(t) + c_6 \mathrm{QBO}_{10}(t)$$

$$+ c_7 \mathrm{QBO}_{30}(t) + c_8 \mathrm{ENSO}(t) + c_9 \mathrm{NAO}(t) + r(t) \quad (2)$$

The results are given as a % of the respective 2000-2010 mean. The proxies used represent sources of geophysical variability with known influence on stratospheric ozone, including the quasi-biennial oscillation (QBO at 30 hPa and 10 hPa), the 10.7 cm solar radio flux describing the 11-year solar cycle (SOL), the El Niño Southern Oscillation (ENSO), the North Atlantic Oscillation (NAO), and Fourier components representing the seasonal cycle (annual and semi-annual variations). t is in months, $r(t)$ is the residual ~~noise~~, c_0 the linear component (the trend), and a the ordinate intercept of the regression line. The data sources for each proxy are provided in the data availability section at the end of this paper.

Stratospheric trends (below 50 km) are derived from data covering 2000 to 2018 while lower mesospheric trends (above 50 km) are derived from data covering 2010 to 2018. The solar cycle proxy has not been considered in the latter case because of the high probability of correlation with the linear slope when regressing timeseries shorter than one solar cycle.

All data points are considered with equal weights, and the uncertainty of the fit parameters is estimated from the regression residuals. Residual autocorrelations are removed using the Cochrane–Orcutt transformation (Cochrane and Orcutt, 1949).

4 Results

4.1 Validation

Since the ozone profile time series used in this study is retrieved with an updated version of the OEM Arts/Qpack retrieval (see subsection 2.1), we carried out a new validation of the Payerne MWR dataset with ground-based and satellites ozone profile measurements.

4.1.1 Profiles of the mean relative differences

Individual Payerne MWR ozone profiles were compared with coincident satellite ozone profiles with a maximal temporal separation of 2h. The means of the relative differences between each satellite dataset and the Payerne MWR are plotted for the 25-65 km altitude range in Fig. 4a for daytime (10:00 LST–14:00 LST) and Fig. 4b for nighttime (22:00 LST–2:00 LST). The comparison with the HALOE sunset dataset is plotted on the daytime panel and the HALOE sunrise dataset on the nighttime panel, but these should be considered with caution given the low number of coincident measurements. The dotted lines represent the standard errors of the means.

The spread of the relative differences are as large as ±12%. Similar differences (i.e. ±5% to ±10%) are reported in studies comparing satellite datasets (Laeng et al., 2014; Rahpoe et al., 2015) and comparing ground-based and satelite datasets (Hubert et al., 2016).

https://doi.org/10.5194/acp-2020-101
Preprint. Discussion started: 17 February 2020


Atmospheric Chemistry and Physics Discussions

The mean relative difference of daytime profiles compared to MLS is approximately between -8 and +8% over the 30–65 km altitude range, while the relative difference compared to the HARMOZ datasets is between -10% and +10% over the 30–65 km altitude range. A systematic positive bias of the MIPAS, GBL, GOMOS, SCIAMACHY, HALOE and Bern MWR day and night datasets compared with the Payerne MWR is reported below 30 km. The larger relative difference compared to the HARMOZ datasets (when compared to the 5% difference with MLS) can be explained by the choice of the spatial coincidence criteria. The criteria for spatial coincidence (10° by 10°) may seem large but is necessary given the smaller number of coincidences. Reducing the spatial coincidence criterion from 10° to 6° in latitude reduces the number of matches by more than 50%. However, the spatial distribution of matches is uneven, with a large number on the north and south borders of the box. This induces a larger bias, given the ozone gradient at these latitudes. The high density of the MLS measurements means a reduced area can be used for the spatial coincidence criteria without degrading the statistics.

Below 48km, the nighttime differences compared to MLS, GOMOS, and MIPAS are within ±5%. Above 50km, the relative differences are as large as -7% compared to MLS and -15% compared to MIPAS and GOMOS. The Payerne MWR overestimates nighttime ozone at 55 km compared to all the satellite profiles except HALOE. The positive bias at night at 55km was reported by Hocke et al. (2007) for a previous version of the Payerne retrieval. Rüfenacht and Kämpfer (2017) show that the emission signal of the secondary ozone layer can alter the nighttime ozone retrieval and thus the ozone values above 0.2 hPa can be overestimated. The a priori profiles and standard deviations used in the Payerne retrieval are identical for day- and nighttime conditions leading to the effects on the nighttime ozone profiles described in Rüfenacht and Kämpfer (2017), i.e. an overestimation of ozone at 55 km. Considering that the ozone secondary peak intensity is larger at night and that the width of the AVKs of the Payerne MWR dataset is on the order of 17 km in the lower mesosphere, the ozone information in the profile at 55 km is influenced by the ozone content at higher altitudes.

The ±10% agreement of the Payerne MWR with satellites assess the quality of the measurements considering the uncertainties of the respective instruments. The systematic 7% underestimation of ozone at 30 km is under investigation, while the nighttime 15% overestimation has been assigned to a mesospheric aliasing effect. The agreement between the two swiss MWRs is described in the next paragraph.

4.1.1.1 Relative difference compared to the Bern MWR

The mean relative difference between the Bern and Payerne MWRs lies between ±10% up to 40km, increasing up to a maximum of -10 to -13% between 47–57 km. Since the measurement setups of the Bern and Payerne MWRs are very similar we would expect better agreement between the two instruments. However, the Payerne and Bern retrieval procedures differ in the calibration, in the a priori climatology used, as well as in the uncertainties used for the a priori and measurement covariance matrices, the spectroscopic parameters (pressure broadening), and in the temperature profiles used in the forward model. The measurement contribution and total error therefore slightly differ between the two MWRs. Based on a sensitivity study of the retrieval parameters of the Payerne MWR ozone profiles, the influence of the spectroscopic parameters is as high as ±7% at 50 km, while the influence of the forward model temperature profile is between ±2% at 50 km. Moreover, no period weighting to account for anomalous measurements such as described in Bernet et al. (2019) has been applied to the Bern MWR dataset.

https://doi.org/10.5194/acp-2020-101
Preprint. Discussion started: 17 February 2020

Atmospheric Chemistry and Physics Discussions

Efforts are ongoing to harmonize the retrieval processes and it is future work to harmonize the two data processing chains to determine the sources for the differences.

4.1.1.2 Relative difference compared to SOCOL v3.0

The Payerne MWR and SOCOL climatological means agree within 15% at 50km (Fig. 4). Above this level, the daytime values show differences of similar magnitude, but the nighttime differences are much larger, up to 40% at 0.2 hPa (60km). The relative differences also appears to vary with season, with ozone values being closer in NH winter than in summer. The high time resolution of both the Payerne MWR and SOCOL simulations means that it is possible to derive ozone diurnal cycle profiles (Fig. 5). In the NH mid-latitudes, the daytime ozone levels vary with altitude from +4% at 4 hPa (36 km) to -25% at 0.2 hPa (60 km) with respect to nighttime values. The comparison of ozone diurnal cycles measured by the Payerne MWR and simulated by SOCOL v3.0 show good agreement, both with negative values during the day above 0.85 hPa, a minimum at sunrise, and a maximum in the afternoon, peaking at 12 hPa and 4 hPa respectively for Payerne MWR (Fig. 5a and b). The desagreements in amplitude and in height of transition from the lower mesospheric to the stratospheric diurnal cycle mode are slightly reduced when considering the AVK convolution of SOCOL v3.0 profiles to the Payerne MWR vertical resolution. This is due to the degradation of the model information vertical resolution (Fig. 5c) as described in (Studer et al., 2014).

SOCOL v3.0 overestimates the amplitude of the ozone diurnal cycle in the upper and middle (32-10 hPa) stratosphere and this could be related to the known overestimation of water vapor and upward transport in the model as well as to the positive temperature bias compared to ERA-40 (Stenke et al., 2013).

Despite a poor agreement above 50 km, the good agreement between the Payerne MWR and SOCOL v3.0 ozone values in the 30 to 50 km altitude range and moreover in their diurnal variations make it possible to consider the comparison of both datasets variation with LST. Nevertheless, the desagreement in the height of the diurnal cycle extremes has to be considered when comparing trends.

4.2 Multiple linear regression analysis

4.2.1 24-hour, daytime, and nighttime trends

Up to 50 km the 2000-2018 24-hour trend estimates are similar at the 95% confidence level to the 2000-2016 trend profiles of LOTUS NH ground-based datasets (Umkehr, LIDAR below 40 km) and a range of models as described in Petropavlovskikh et al. (2019) (tly positive. For this study, we extended the time range by 2 years. Effects on trends can be noticed below 30 km with a shift towards more p ic trends do not vary significantly. At 50 km, the 24-hour average Payerne MWR trend is 2%/dec lower than the trends calculated from the Dobson Umkehr, satellite, and model datasets used by Petropavlovskikh et al. (2019), which are all positive, but non-significant at that altitude.

daily mean

In Fig. 6, caption is not sufficient (1sig lines?, shaded aera full range or what?) Legend

Please re-arrange: At 2 hPa the trend is with 2%/dec significantly positive.

We tested the effect of the extended time span on the results:

The change of sign in the trend is a hint to understimated

Style: 2%/dec or 2%/10y (see Fig).

Day- and nighttime trends for the 3 MWRs, MLS satellite and SOCOL CCM datasets, are plotted in Fig. 7. The lower panel shows 2000–2016 day- and nighttime trends up to 0.59 hPa (50 km). The upper panel concerns the 2010–2018 day- and

https://doi.org/10.5194/acp-2020-101
Preprint. Discussion started: 17 February 2020


Atmospheric Chemistry and Physics Discussions

nighttime trends in the low mesosphere. The focus here is the comparison of day- and nighttime trend profiles, being obvious that we cannot directly compare 2000-2016 with 2010-2018 trends. Similarly, the MLO MWR trends cannot be compared to the NH trends.

Day- and nighttime mid-stratospheric trends do not differ significantly at the 95% confidence level for the Payerne MWR, SOCOL, MLS satellite, or for the MLO MWR (lower panel of Fig. 7). The largest, but still not statistically significant, difference between day- and nighttime trends is measured at 45 km, with positive trend estimates ranging from 2 to 4%/dec for the Payerne MWR, and from 2 to 5%/dec for MLS. The statistically significant difference measured for the Bern MWR at 50 km is probably artificially produced by the 2009 homogenization which does not take into account the measurement contribution variation and/or a variation of the correction offset with LST. A similar behavior was observed for the Payerne MWR before the comprehensive homogenization of the AOS and FFTS datasets.

No significant differences between trends derived from day- and nighttime measuring instruments can therefore be attributed to a systematic measurement schedule difference between the instruments. As below 45 km, the diurnal cycle amplitude is minimal at sunrise and maximal in the afternoon, we do not expect any influence of the ozone diurnal cycle on the daytime and nighttime long-term trends at these altitudes. The potential influence of the diurnal cycle (ozone morning minimum and afternoon maximum) at these altitudes will be investigated by considering trends for each hour (see Sect. 4.2.2).

Day- and nighttime lower mesospheric trends do not differ significantly at 95% for the Payerne MWR, SOCOL, MLS satellite, or for the MLO MWR (upper panel of Fig. 7). The largest, but still not statistically significant, difference between day- and nighttime trends is measured at 57 km, with trend estimates ranging from 0 to 3%/dec for the Payerne MWR, and at 62 km, with trend estimates ranging from 0 to -2%/dec for MLS. At these altitudes too, no significant differences between trends derived from day- and nighttime measuring instruments can be attributed to a systematic measurement schedule difference, despite the fact that we expected an influence of the ozone diurnal cycle on the trend estimates in this altitude range. The day- and nighttime trends as measured by the Bern MWR are significantly negative in the lower mesosphere. We did not investigate the large negative nighttime trend estimates in this work but, as mentioned in Sect. 4.1.1.1, intensive efforts are ongoing to homogenise the two swiss MWRs for the post-2010 period.

4.2.2 Payerne MWR ozone trends as a function of LST

In the stratosphere the ozone diurnal cycle shows presents a minimum at sunrise (∼12.5 hPa) and a maximum (∼4.16 hPa) in the afternoon (shown in Fig. 5). Long-term trends for each hour of the day were calculated using the method described in Sect. 3.2. This is only possible for the Payerne and Bern MWR datasets and for the SOCOL v3.0 simulations, which all have the necessary hourly time resolution.

In Fig. 8, one trend estimate in %/dec is plotted for each pressure level in the stratosphere and each hour of the day without any interpolation. Trend profiles in %/dec are shown as a function of LST, with hatches indicating values which are not significantly different from zero at the 95% confidence level. The Payerne MWR mid-stratospheric 2000-2018 trends are represented in Fig. 8a and Bern MWR trends in Fig. 8b. For each pressure level, the variations of ozone trends as a function of LST are small and the differences are not significant at the 95% confidence level. The largest, but still not statistically

https://doi.org/10.5194/acp-2020-101
Preprint. Discussion started: 17 February 2020


Atmospheric Chemistry and Physics Discussions

significant, difference is shown between 4 and 14 h LST at 40 km (Fig. 8c in red). Even when considering the altitude difference between the morning minimum and the afternoon maximum, the long-term ozone trends at the morning minimum (12.5 hPa, 8h LST, in blue) is similar to the long-term ozone trends at the afternoon maximum (4.16 hPa and 14h LST, in black) at the 95% confidence level.

4.2.3 SOCOL OH, NOx and temperature trends as a function of LST

Based on the correlation between ~~the~~ stratospheric O3 and ~~the~~ NOx, the active H and the Temperature long-term variations, and on the similarities of the ozone diurnal variation simulated by SOCOL and measured by the Payerne MWR, we investigate the variation of the NOx, OH and T trends with LST as an attempt to derive a correlation between ozone trend variation with LST and ozone-influencing substances trends variations with LST. We derive trends of simulated OH, NOx and T as a function of LST in the stratosphere. We apply a similar MLR with proxies for the solar cycle, QBO at 30 hPa and 10 hPa, ENSO MEI and aerosols to monthly mean values for the 2000-2016 period.

Figure 9a shows the linear trends as a function of ??? of LST. SOCOL shows a positive OH trend of 4%/dec during the day and a non significant trend of -2%/dec at night. No significant variation of daytime OH trend with LST is seen in the stratosphere. The OH impact on ozone chemistry in this altitude range is very limited when compared to NOx and Cl (Schanz, 2015). Active H influence increases from 0.3 hPa up, but is negligible at pressure levels lower than 2 hPa. During the night, OH disappears rather fast due to the absence of photolysis (OH production) and large OH reactivity (OH loss). The nighttime chemistry is mainly influenced by temperature, thus the nighttime ozone trend simulated by SOCOL should be related to the temperature trends (Fig. 9c) b) and not to the OH trends.

Figure 9b shows the temperature trends as a function of LST. SOCOL shows a slightly negative trend of -1%/dec for both day- and nighttime between 30 km and 43 km. The negative trends are not significant out of this altitude range. Here again, no significant variation of temperature trend with LST is reported. We can only report a negative correlation between the negative temperature trend and the positive ozone trend independent of LST.

In the stratosphere, NOx variability plays a key role in ozone changes (Hendrick et al., 2012; Nedoluha et al., 2015a) with a maximum influence at 4 hPa. A MLR with proxies for the solar cycle, the QBO at 30 hPa and at 10 hPa was applied to monthly means of SOCOL simulated reactive NOx (NOx =NO+NO2) for the period 2000-2016. Figure 9d shows the linear trends in simulated NOx as a function of LST. SOCOL shows a negative trend of -3%/dec in the morning and a statistically non-significant negative trend of -1%/dec in the afternoon. The variation with LST is again not significant at the 95% confidence level. The simulated NOx trends are agree with those reported by Hendrick et al. (2012), who shows negative trends of the NOx column for 24h-average datasets. Nedoluha et al. (2015b) demonstrated using HALOE (1991-2005) and MLS (2004-2013) measurements that a significant decrease in ozone near 10 hPa in the tropics could be related to a spatially localized, but long-term increase in NOx. Although they also showed that the response of ozone to NOx chemistry varies strongly with time of day (Nedoluha et al., 2015a), with ozone destruction through the NOx cycle increasing from the morning to the afternoon (Schanz, 2015). Here we report negative trends in the morning and in the afternoon, but their difference is not significant at the

https://doi.org/10.5194/acp-2020-101
Preprint. Discussion started: 17 February 2020


Atmospheric Chemistry and Physics Discussions

95% confidence level. However, when we consider just the global trends without any distinction by LST, we can see a similar negative correlation between the negative NOx trend and the positive O3 trend.

5 Conclusions

The 2000-2018 Payerne MWR dataset has been reprocessed and harmonized to ensure a constant measurement contribution to the ozone profiles and to take into account the effects of the three major technical upgrades (2001, 2005, and 2009). The dataset agrees now within $\pm 5\%$ with MLS over the 30 to 65 km altitude range and within $\pm 10\%$ of the HARMOZ satellite datasets over the 30 to 65 km altitude range. The Payerne MWR agrees within $\pm 15\%$ up to 50 km with the SOCOL v3.0 CCM. We report a 15% mean positive offset of the Payerne MWR datasets compared to other datasets at nighttime in the lower mesosphere. The overestimated nighttime ozone of the Payerne MWR is caused by an aliasing of the mesospheric nighttime ozone signal into the lower mesospheric ozone signal. Post-2000 long-term trends were calculated using MLR applied to the global Payerne MWR dataset and results agree well with other NH ground-based instrument trends published in Petropavlovskikh et al. (2019). this statement is a little bit misleading: trend changes its sign! Adding two more years to the dataset was shown to increase the trends below 30 km. A MLR was also applied to the high resolution data to assess whether significant trends could be detected in the ozone diurnal cycle. Neither stratospheric nor lower mesospheric ozone trends vary with LST significantly at the 95% confidence level. No significant long-term variation of the amplitude of the diurnal cycle is observed even if we consider the altitude difference of the ozone diurnal cycle minimum and maximum. Without any significant variation of the ozone trend with LST, no correlation is possible with the LST variation of temperature, OH and NO_x trends. We can only report a negative correlation between the negative NOx trend, the negative temperature trend and the positive ozone trend independent of LST in the stratosphere. From our quantification of the ozone trends as a function of LST we conclude, that systematic sampling differences between instruments cannot explain significant differences in trend estimates for the 2000-2018 period in the stratosphere and for the 2010-2018 period in the mesosphere.

Data availability. The most recent version of the Payerne MWR dataset will be available in the NDACC database at http://ftp.cpc.ncep.noaa.gov/ndacc/station/payerne/ames/mwave.
The Bern and Mauna Loa MWR datasets used for this study are available at http://ftp.cpc.ncep.noaa.gov/ndacc/station/bern/hdf/mwave and http://ftp.cpc.ncep.noaa.gov/ndacc/station/maunaloa/hdf/mwave.
The HARMOZ satellite datasets are available from ftp://ftp-ae.oma.be/esacci/ozone/Limb_Profiles/L2/HARMOZ_PRS.
The MLS ozone dataset is available from the NASA Goddard Space Flight Center Earth Sciences Data and Information Services Center (GES DISC) at http://disc.sci.gsfc.nasa.gov/Aura/data-holdings/MLS/index.shtml.
The sources for the proxy data used in the MLR are provided in Table 1.

Author contributions. EMB was responsible for the ground-based ozone measurements with the Payerne MWR, performed the data analysis and prepared the manuscript. AH and RR contributed to the interpretation of the results. LN provided the code for the trend calculations

https://doi.org/10.5194/acp-2020-101
Preprint. Discussion started: 17 February 2020

Atmospheric Chemistry and Physics Discussions

as function of LST. FT, WTB and EVR provided the SOCOL v3.0 dataset. KH, NK and LB were responsible for ground-based ozone measurements with the Bern MWR. IB and GN were responsible for ground-based ozone measurements with the MLO MWR. All co-authors contributed to the manuscript preparation.

Competing interests. The authors have no competing interests.

Acknowledgements. This work has been funded by MeteoSwiss within the Swiss Global Atmospheric Watch (GAW) program of the World Meteorological Organization. WTB was funded by SNSF projects 200020_163206 (SIMA) and 200020_182239 (POLE).

https://doi.org/10.5194/acp-2020-101
Preprint. Discussion started: 17 February 2020

Atmospheric Chemistry and Physics Discussions

References

Ball, W. T., Alsing, J., Mortlock, D. J., Rozanov, E. V., Tummon, F., and Haigh, J. D.: Reconciling differences in stratospheric ozone composites, Atmospheric Chemistry and Physics, 17, 12 269–12 302, https://doi.org/10.5194/acp-17-12269-2017, 2017.

Ball, W. T., Alsing, J., Mortlock, D. J., Staehelin, J., Haigh, J. D., Peter, T., Tummon, F., Stübi, R., Stenke, A., Anderson, J., Bourassa, A., Davis, S. M., Degenstein, D., Frith, S., Froidevaux, L., Roth, C., Sofieva, V., Wang, R., Wild, J., Yu, P., Ziemke, J. R., and Rozanov, E. V.: Evidence for a continuous decline in lower stratospheric ozone offsetting ozone layer recovery, Atmospheric Chemistry and Physics, 18, 1379–1394, https://doi.org/10.5194/acp-18-1379-2018, 2018.

Ball, W. T., Alsing, J., Staehelin, J., Davis, S. M., Froidevaux, L., and Peter, T.: Stratospheric ozone trends for 1985-2018: sensitivity to recent large variability, Atmospheric Chemistry and Physics, 19, 12 731—12 748, https://doi.org/10.5194/acp-19-12731-2019, 2019.

Barnett, J. J., Houghton, J. T., and Pyle, J. A.: The temperature dependence of the ozone concentration near the stratopause, Quarterly Journal of the Royal Meteorological Society, 101, 245–257, https://doi.org/10.1002/qj.49710142808, 1975.

Bernet, L., von Clarmann, T., Godin-Beekmann, S., Ancellet, G., Maillard Barras, E., Stübi, R., Steinbrecht, W., Kämpfer, N., and Hocke, K.: Ground-based ozone profiles over central Europe: incorporating anomalous observations into the analysis of stratospheric ozone trends, Atmospheric Chemistry and Physics, 19, 4289–4309, https://doi.org/10.5194/acp-19-4289-2019, 2019.

Bertaux, J. L., Kyrölä, E., Fussen, D., Hauchecorne, A., Dalaudier, F., Sofieva, V., Tamminen, J., Vanhellemont, F., Fanton d'Andon, O., Barrot, G., Mangin, A., Blanot, L., Lebrun, J. C., Pérot, K., Fehr, T., Saavedra, L., Leppelmeier, G. W., and Fraisse, R.: Global ozone monitoring by occultation of stars: an overview of GOMOS measurements on ENVISAT, Atmospheric Chemistry and Physics, 10, 12 091–12 148, https://doi.org/10.5194/acp-10-12091-2010, 2010.

Bovensmann, H., Burrows, J. P., Buchwitz, M., Frerick, J., Noël, S., Rozanov, V. V., Chance, K. V., and Goede, A. P. H.: SCIAMACHY: Mission Objectives and Measurement Modes, Journal of the Atmospheric Sciences, 56, 127–150, https://doi.org/10.1175/1520-0469(1999)056<0127:SMOAMM>2.0.CO;2, 1999.

Buehler, S., Eriksson, P., Kuhn, T., von Engeln, A., and Verdes, C.: ARTS, the atmospheric radiative transfer simulator, Journal of Quantitative Spectroscopy and Radiative Transfer, 91, 65–93, https://doi.org/10.1016/j.jqsrt.2004.05.051, 2005.

Calisesi, Y.: Monitoring of stratospheric and mesospheric ozone with a ground-based microwave radiometer: data retrieval, analysis, and applications, Ph.D. thesis, Philosophisch- Naturwissenschaftliche Fakultät, Universität Bern, Bern, Switzerland, 77 pp., http://www.iap.unibe.ch/publications, 2000.

Chang, J. S., Brost, R. A., Isaksen, I. S. A., Madronich, S., Middleton, P., Stockwell, W. R., and Walcek, C. J.: A three-dimensional Eulerian acid deposition model: Physical concepts and formulation, Journal of Geophysical Research, 92, 14 681–14 700, https://doi.org/10.1029/JD092iD12p14681, 1987.

Chipperfield, M. P., Bekki, S., Dhomse, S., Neil, R. P., Hassler, B., Hossaini, R., Steinbrecht, W., Thiéblemont, R., and Weber, M.: Detecting recovery of the stratospheric ozone layer, Nature Publishing Group, 549, 211–218, https://doi.org/10.1038/nature23681, 2017.

Chubachi, S.: A special ozone observation at Syowa Station, Antarctica from February 1982 to January 1983, in: Atmospheric Ozone, pp. 285–289, https://doi.org/10.1007/978-94-009-5313-0_58, 1985.

Cochrane, D. and Orcutt, G. H.: Application of least squares regression to relationships containing auto-correlated error terms, J. Am. Stat. Assoc., 44, 32–61, 1949.

Connor, B. J., A., P., Tsou, J. J., and McCormick, P.: during measurements, Journal of Geophysical Research, 100, 9283–9291, 1995.

https://doi.org/10.5194/acp-2020-101
Preprint. Discussion started: 17 February 2020

Atmospheric Chemistry and Physics Discussions

Craig, R. A. and Ohring, G.: The Temperature dependence of ozone radiational heating Rates in the vicinity of the mesopeak, Journal of Meteorology, 15, 59–62, https://doi.org/10.1175/1520-0469(1958)015<0059:TTDOOR>2.0.CO;2, 1958.

Damadeo, R. P., Zawodny, J. M., Remsberg, E. E., and Walker, K. A.: The Impact of Non-uniform Sampling on Stratospheric Ozone Trends Derived from Occultation Instruments, Atmospheric Chemistry and Physics, 18, 535—554, https://doi.org/10.5194/acp-18-535-2018, 2018.

E., G., Rozanov, A., Chipperfield, M., Dhomse, S., Weber, M., Arosio, C., Feng, W., and Burrows, J.: Dynamically controlled ozone decline in the tropical mid-stratosphere observed by SCIAMACHY, Atmospheric Chemistry and Physics, 19, 767–783, https://doi.org/10.5194/acp-19-767-2019, 2019.

Egorova, T. A., Rozanov, E. V., Zubov, V. A., and Karol, I. L.: Model for investigating ozone trends (MEZON), Izv. Atmos. Ocean. Phys., 39, 277–292, 2003.

Eriksson, P., Jiménez, C., and Buehler, S. A.: Qpack, a general tool for instrument simulation and retrieval work, Journal of Quantitative Spectroscopy and Radiative Transfer, 91, 47–64, https://doi.org/10.1016/j.jqsrt.2004.05.050, 2005.

Eyring, V., Cionni, I., Bodeker, G. E., Charlton-Perez, A. J., Kinnison, D. E., Scinocca, J. F., Waugh, D. W., Akiyoshi, H., Bekki, S., Chipperfield, M. P., Dameris, M., Dhomse, S., Frith, S. M., Garny, H., Gettelman, A., Kubin, A., Langematz, U., Mancini, E., Marchand, M., Nakamura, T., Oman, L. D., Pawson, S., Pitari, G., Plummer, D. A., Rozanov, E., Shepherd, T. G., Shibata, K., Tian, W., Braesicke, P., Hardiman, S. C., Lamarque, J. F., Morgenstern, O., Pyle, J. A., Smale, D., and Yamashita, Y.: Multi-model assessment of stratospheric ozone return dates and ozone recovery in CCMVal-2 models, Atmospheric Chemistry and Physics, 10, 9451–9472, https://doi.org/10.5194/acp-10-9451-2010, 2010.

Farman, J. C., Gardiner, B. G., and Shanklin, J. D.: Large losses of total ozone in Antartica reveal seasonal ClOx/NOx interaction, Nature, 315, 207–210, 1985.

Flury, T., Hocke, K., Haefele, A., Kämpfer, N., and Lehmann, R.: Ozone depletion, water vapor increase, and PSC generation at midlatitudes by the 2008 major stratospheric warming, Journal of Geophysical Research Atmospheres, 114, 1–14, https://doi.org/10.1029/2009JD011940, 2009.

Giorgetta, M., Manzini, E., Roeckner, E., Esch, M., and Bengtsson, L.: Climatology and forcing of the quasi-biennial oscillation in the MAECHAM5 model, J. Climate, 19, 3882–3901, https://doi.org/10. 1175/JCLI3830.1, 2006.

Haefele, A., Hocke, K., Kämpfer, N., Keckhut, P., Marchand, M., Bekki, S., Morel, B., Egorova, T., and Rozanov, E.: Diurnal changes in middle atmospheric H2O and O3 : Observations in the Alpine region and climate models, Journal of Geophysical Research, 113, D17 303, https://doi.org/10.1029/2008JD009892, 2008.

Hendrick, F., Mahieu, E., Bodeker, G. E., Boersma, K. F., Chipperfield, M. P., De Mazière, M., De Smedt, I., Demoulin, P., Fayt, C., Hermans, C., Kreher, K., Lejeune, B., Pinardi, G., Servais, C., Stübi, R., Van Der A, R., Vernier, J. P., and Van Roozendael, M.: Analysis of stratospheric NO2 trends above Jungfraujoch using ground-based UV-visible, FTIR, and satellite nadir observations, Atmospheric Chemistry and Physics, 12, 8851–8864, https://doi.org/10.5194/acp-12-8851-2012, 2012.

Hocke, K., Kämpfer, N., Ruffieux, D., Froidevaux, L., Parrish, A., Boyd, I., von Clarmann, T., Steck, T., Timofeyev, Y. M., Polyakov, A. V., and Kyrölä, E.: Comparison and synergy of stratospheric ozone measurements by satellite limb sounders and the ground-based microwave radiometer SOMORA, Atmospheric Chemistry and Physics, 7, 4117–4131, https://doi.org/10.5194/acp-7-4117-2007, 2007.

Hubert, D.: The temporal and spatial homogeneity of ozone profile data records obtained by ozonesonde, lidar and microwave radiometer networks, in preparation, 2019.

https://doi.org/10.5194/acp-2020-101
Preprint. Discussion started: 17 February 2020

Atmospheric Chemistry and Physics Discussions

Hubert, D., Lambert, J. C., Verhoelst, T., Granville, J., Keppens, A., Baray, J. L., Bourassa, A. E., Cortesi, U., Degenstein, D. A., Froidevaux, L., Godin-Beekmann, S., Hoppel, K. W., Johnson, B. J., Kyrölä, E., Leblanc, T., Lichtenberg, G., Marchand, M., McElroy, C. T., Murtagh, D., Nakane, H., Portafaix, T., Querel, R., Russell, J. M., Salvador, J., Smit, H. G., Stebel, K., Steinbrecht, W., Strawbridge, K. B., Stübi, R., Swart, D. P., Taha, G., Tarasick, D. W., Thompson, A. M., Urban, J., Van Gijsel, J. A., Van Malderen, R., Von Der Gathen, P., Walker, K. A., Wolfram, E., and Zawodny, J. M.: Ground-based assessment of the bias and long-term stability of 14 limb and occultation ozone profile data records, Atmospheric Measurement Techniques, 9, 2497–2534, https://doi.org/10.5194/amt-9-2497-2016, 2016.

Keating, G. M., Pitts, M. C., and Young, D. F.: Ozone reference models for the middle atmosphere, Advances in Space Research, 10, 317–355, https://doi.org/10.1016/0273-1177(90)90404-N, 1990.

Kyrölä, E., Tamminen, J., Sofieva, V., Bertaux, J. L., Hauchecorne, A., Dalaudier, F., Fussen, D., Vanhellemont, F., Fanton d'Andon, O., Barrot, G., Guirlet, M., Mangin, A., Blanot, L., Fehr, T., Saavedra de Miguel, L., and Fraisse, R.: Retrieval of atmospheric parameters from GOMOS data, Atmospheric Chemistry and Physics, 10, 11 881–11 903, https://doi.org/10.5194/acp-10-11881-2010, 2010.

Kyrölä, E., Laine, M., Sofieva, V., Tamminen, J., Pivrinta, S. M., Tukiainen, S., Zawodny, J., and Thomason, L.: Combined SAGE II-GOMOS ozone profile data set for 1984-2011 and trend analysis of the vertical distribution of ozone, Atmospheric Chemistry and Physics, 13, 10 645–10 658, https://doi.org/10.5194/acp-13-10645-2013, 2013.

Laeng, A., Grabowski, U., Von Clarmann, T., Stiller, G., Glatthor, N., Höpfner, M., Kellmann, S., Kiefer, M., Linden, A., Lossow, S., Sofieva, V., Petropavlovskikh, I., Hubert, D., Bathgate, T., Bernath, P., Boone, C. D., Clerbaux, C., Coheur, P., Damadeo, R., Degenstein, D., Frith, S., Froidevaux, L., Gille, J., Hoppel, K., Mchugh, M., Kasai, Y., Lumpe, J., Rahpoe, N., Toon, G., Sano, T., Suzuki, M., Tamminen, J., Urban, J., Walker, K., Weber, M., and Zawodny, J.: Validation of MIPAS IMK/IAA V5R-O3-224 ozone profiles, Atmospheric Measurement Techniques, 7, 3971–3987, https://doi.org/10.5194/amt-7-3971-2014, 2014.

Laeng, A., von Clarmann, T., Stiller, G., Dinelli, B. M., Dudhia, A., Raspollini, P., Glatthor, N., Grabowski, U., Sofieva, V., Froidevaux, L., Walker, K. A., and Zehner, C.: Merged ozone profiles from four MIPAS processors, Atmospheric Measurement Techniques, 10, 1511–1518, https://doi.org/10.5194/amt-10-1511-2017, 2017.

Lin, S. J. and Rood, R. B.: Multidimensional flux-form semi-Lagrangian transport schemes, Mon. Wea. Rev., 124, 2046–2070, 1996.

Livesey, N. J.: Earth Observing System (EOS) Aura Microwave Limb Sounder (MLS) Version 4.2x Level 2 data quality and description document, pp. 1–168, https://mls.jpl.nasa.gov/data/v4-2_data_quality_document.pdf, 2018.

Lossow, S., Khosrawi, F., Kiefer, M., Walker, K. A., Bertaux, J.-l., Blanot, L., Russell, J. M., Remsberg, E. E., Gille, J. C., Sugita, T., Sioris, C. E., Dinelli, B. M., Papandrea, E., Raspollini, P., Garcia-Comas, M., Stiller, G. P., von Clarmann, T., Dudhia, A., Read, W. G., Nedoluha, G. E., Damadeo, R. P., Zawodny, J. M., Weigel, K., Rozanov, A., Azam, F., Bramstedt, K., Noël, S., Burrows, J. P., Sagawa, H., Kasai, Y., Urban, J., Eriksson, P., Murtagh, D. P., Hervig, M. E., Högberg, C., Hurst, D. F., and Rosenlof, K. H.: The SPARC water vapour assessment II: Profile-to-profile comparisons of stratospheric and lower mesospheric water vapour data sets obtained from satellites, Atmospheric Measurement Techniques, 12, 2693—-2732, https://doi.org/10.5194/amt-12-2693-2019, 2019.

Mäder, J. A., Staehelin, J., Peter, T., Brunner, D., Rieder, H. E., and Stahel, W. A.: Evidence for the effectiveness of the Montreal Protocol to protect the ozone layer, Atmospheric Chemistry and Physics, 10, 12 161–12 171, https://doi.org/10.5194/acp-10-12161-2010, 2010.

Maillard Barras, E., Haefele, A., Stübi, R., and Ruffieux, D.: A method to derive the Site Atmospheric State Best Estimate (SASBE) of ozone profiles from radiosonde and passive microwave data, Atmospheric Measurement Techniques Discussions, 8, 3399–3422, https://doi.org/10.5194/amtd-8-3399-2015, 2015.

Marsh, D., Smith, A., and Noble, E.: Mesospheric ozone response to changes in water vapor, Journal of Geophysical Research: Atmospheres, 108, 4109, https://doi.org/10.1029/2002JD002705, 2003.

https://doi.org/10.5194/acp-2020-101
Preprint. Discussion started: 17 February 2020

Atmospheric Chemistry and Physics Discussions

McPeters, R. D. and Labow, G. J.: Climatology 2011: An MLS and sonde derived ozone climatology for satellite retrieval algorithms, Journal of Geophysical Research Atmospheres, 117, https://doi.org/10.1029/2011JD017006, 2012.

Meul, S., Dameris, M., Langematz, U., Abalichin, J., Kerschbaumer, A., Kubin, A., and Oberländer-Hayn, S.: Impact of rising greenhouse gas concentrations on future tropical ozone and UV exposure, Geophysical Research Letters, 43, 2919–2927, https://doi.org/10.1002/2016GL067997, 2016.

Molina, M. J. and S., R. F.: Stratospheric sink for chlorofluoromethanes: chlorine atom-catalysed destruction of ozone, Nature Geoscience, 249, 810–812, 1974.

Moreira, L., Hocke, K., Eckert, E., Von Clarmann, T., and Kämpfer, N.: Trend analysis of the 20-year time series of stratospheric ozone profiles observed by the GROMOS microwave radiometer at Bern, Atmospheric Chemistry and Physics, 15, 10 999–11 009, https://doi.org/10.5194/acp-15-10999-2015, 2015.

Nedoluha, G. E., Boyd, I. S., Parrish, A., Gomez, R. M., Allen, D. R., Froidevaux, L., Connor, B. J., and Querel, R. R.: Unusual stratospheric ozone anomalies observed in 22 years of measurements from Lauder, New Zealand, Atmospheric Chemistry and Physics, 15, 6817–6826, https://doi.org/10.5194/acp-15-6817-2015, 2015a.

Nedoluha, G. E., Siskind, D. E., Lambert, A., and Boone, C.: The decrease in mid-stratospheric tropical ozone since 1991, Atmospheric Chemistry and Physics, 15, 4215–4224, https://doi.org/10.5194/acp-15-4215-2015, 2015b.

Newnham, D. A., Clilverd, M. A., Kosch, M., Seppälä, A., and Verronen, P. T.: Simulation study for ground-based Ku-band microwave observations of ozone and hydroxyl in the polar middle atmosphere, Atmospheric Measurement Techniques, 12, 1375–1392, https://doi.org/10.5194/amt-12-1375-2019, 2019.

Pallister, R. C. and Tuck, A. F.: The diurnal variation of ozone in the upper stratosphere as a test of photochemical theory, Quarterly Journal of the Royal Meteorological Society, 109, 271–284, https://doi.org/10.1002/qj.49710946002, 1983.

Parrish, A., Connor, B. J., Tsou, J. J., McDermid, I. S., and Chu, W. P.: Ground-based microwave monitoring of stratospheric ozone, Journal of Geophysical Research, 97, 2541, https://doi.org/10.1029/91JD02914, 1992.

Parrish, A., Boyd, I. S., Nedoluha, G. E., Bhartia, P. K., Frith, S. M., Kramarova, N. A., Connor, B. J., Bodeker, G. E., Froidevaux, L., Shiotani, M., and Sakazaki, T.: Diurnal variations of stratospheric ozone measured by ground-based microwave remote sensing at the Mauna Loa NDACC site: Measurement validation and GEOSCCM model comparison, Atmospheric Chemistry and Physics, 14, 7255–7272, https://doi.org/10.5194/acp-14-7255-2014, 2014.

Parrish, A. D.: Millimeter-wave remote sensing of ozone and trace constituents in the stratosphere, Proc. IEEE, 82, 1915–1929, 1994.

Petropavlovskikh, I., Godin-Beekmann, S., Hubert, D., Damadeo, R. P., Hassler, B., Sofieva, V. F., Frith, S. M., and Tourpali, K.: SPARC/IOC/GAW report on Long-term Ozone Trends and Uncertainties in the Stratosphere, Report No. 9, GAW Report No. 241, WCRP-17/2018, https://doi.org/10.17874/f899e57a20b, 2019.

Poeschl, U., von Kuhlmann, R., Poisson, N., and Crutzen, P. J.: Development and intercomparison of condensed isoprene oxidation mechanisms for global atmospheric modeling, J. Atmos. Chem., 37, 29–52, https://doi.org/10.1023/A:1006391009798, 2000.

Rahpoe, N., Weber, M., Rozanov, A. V., Weigel, K., Bovensmann, H., Burrows, J. P., Laeng, A., Stiller, G., Von Clarmann, T., Kyrölä, E., Sofieva, V. F., Tamminen, J., Walker, K., Degenstein, D., Bourassa, A. E., Hargreaves, R., Bernath, P., Urban, J., and Murtagh, D. P.: Relative drifts and biases between six ozone limb satellite measurements from the last decade, Atmospheric Measurement Techniques, 8, 4369–4381, https://doi.org/10.5194/amt-8-4369-2015, 2015.

https://doi.org/10.5194/acp-2020-101
Preprint. Discussion started: 17 February 2020

Atmospheric Chemistry and Physics Discussions

Revell, L. E., Tummon, F., Stenke, A., Sukhodolov, T., Coulon, A., Rozanov, E., Garny, H., Grewe, V., and Peter, T.: Drivers of the tropospheric ozone budget throughout the 21st century under the medium-high climate scenario RCP 6.0, Atmospheric Chemistry and Physics, 15, 5887–5902, https://doi.org/10.5194/acp-15-5887-2015, 2015.

Ricaud, P., de La Noë, J., Connor, B. J., Froidevaux, L., Waters, J. W., Harwood, R. S., MacKenzie, I. A., and Peckham, G. E.: Diurnal variability of mesospheric ozone as measured by the UARS microwave limb sounder instrument: Theoretical and ground-based validations, Journal of Geophysical Research: Atmospheres, 101, 10 077–10 089, https://doi.org/10.1029/95JD02841, 1996.

Rodgers, C. D.: Inverse Methods for Atmospheric Sounding - Theory and Practice, vol. 2 of *Series on Atmospheric Oceanic and Planetary Physics*, World Scientific Publishing Co. Pte. Ltd., Singapore, https://doi.org/10.1142/9789812813718, http://ebooks.worldscinet.com/ISBN/9789812813718/9789812813718.html, 2000.

Roeckner, E., Bäuml, G., Bonaventura, L., Brokopf, R., Esch, M., Giorgetta, M., Hagemann, S., Kirchner, I., Kornblueh, L., Manzini, E., Rhodin, A., Schlese, U., Schulzweida, U., and Tompkins, A.: The atmospheric general circulation model ECHAM 5.PART I: Model description, Tech. Rep., 349, 2003.

Rozanov, E., Calisto, M., Egorova, T., Peter, T., and Schmutz, W.: Influence of the precipitating energetic particles on atmospheric chemistry and climate, Surveys in Geophysics, 33, 483–501, https://doi.org/10.1007/s10712-012-9192-0, 2012.

Rüfenacht, R. and Kämpfer, N.: The importance of signals in the Doppler broadening range for middle-atmospheric microwave wind and ozone radiometry, Journal of Quantitative Spectroscopy and Radiative Transfer, 199, 77–88, https://doi.org/10.1016/j.jqsrt.2017.05.028, 2017.

Russell, J. M., Gordley, L. L., Park, J. H., Drayson, S. R., Hesketh, W. D., Cicerone, R. J., Tuck, A. F., Frederick, J. E., Harries, J. E., and Crutzen, P. J.: The Halogen Occultation Experiment, Journal of Geophysical Research, 98, 10 777–10 797, https://doi.org/10.1029/93JD00799, 1993.

Sander, S. P. e. a.: Chemical Kinetics and Photochemical Data for Use in Atmospheric Studies, Evaluation No. 17, Jet Propulsion Laboratory Publication, 10–6, http://jpldataeval.jpl.nasa.gov, 2011.

Schanz, A., Hocke, K., and Kämpfer, N.: Daily ozone cycle in the stratosphere: Global, regional and seasonal behaviour modelled with the Whole Atmosphere Community Climate Model, Atmospheric Chemistry and Physics, 14, 7645–7663, https://doi.org/10.5194/acp-14-7645-2014, 2014.

Schanz, A. U.: The diurnal variation in middle-atmospheric ozone : simulation and intercomparison, Ph.D. thesis, Philosophisch- Naturwissenschaftliche Fakultät, Universität Bern, Bern, Switzerland, 111 pp., http://www.iap.unibe.ch/publications, 2015.

Sofieva, V. F., Rahpoe, N., Tamminen, J., Kyrölä, E., Kalakoski, N., Weber, M., Rozanov, A., Von Savigny, C., Laeng, A., von Clarmann, T., Stiller, G., Lossow, S., Degenstein, D., Bourassa, A., Adams, C., Roth, C., Lloyd, N., Bernath, P., Hargreaves, R. J., Urban, J., Murtagh, D., Hauchecorne, A., Dalaudier, F., Van Roozendael, M., Kalb, N., and Zehner, C.: Harmonized dataset of ozone profiles from satellite limb and occultation measurements, Earth System Science Data, 5, 349–363, https://doi.org/10.5194/essd-5-349-2013, 2013.

Sofieva, V. F., Ialongo, I., Hakkarainen, J., Kyrölä, E., Tamminen, J., Laine, M., Hubert, D., Hauchecorne, A., Dalaudier, F., Bertaux, J. L., Fussen, D., Blanot, L., Barrot, G., and Dehn, A.: Improved GOMOS/Envisat ozone retrievals in the upper troposphere and the lower stratosphere, Atmospheric Measurement Techniques, 10, 231–246, https://doi.org/10.5194/amt-10-231-2017, 2017.

Solomon, S.: Stratospheric ozone depletion: A review of concepts and history, Reviews of Geophysics, 37, 275–316, https://doi.org/10.1029/1999RG900008, 1999.

Staehelin, J., Tummon, F., Revell, L., Stenke, A., and Peter, T.: Tropospheric Ozone at Northern Mid-Latitudes: Modeled and Measured Long-Term Changes, Atmosphere, 8, 163, https://doi.org/10.3390/atmos8090163, 2017.

https://doi.org/10.5194/acp-2020-101
Preprint. Discussion started: 17 February 2020

690 Steinbrecht, W., Froidevaux, L., Fuller, R., Wang, R., Anderson, J., Roth, C., Bourassa, A., Degenstein, D., Damadeo, R., Zawodny, J., Frith, S., McPeters, R., Bhartia, P., Wild, J., Long, C., Davis, S., Rosenlof, K., Sofieva, V., Walker, K., Rahpoe, N., Rozanov, A., Weber, M., Laeng, A., von Clarmann, T., Stiller, G., Kramarova, N., Godin-Beekmann, S., Leblanc, T., Querel, R., Swart, D., Boyd, I., Hocke, K., Kämpfer, N., Maillard Barras, E., Moreira, L., Nedoluha, G., Vigouroux, C., Blumenstock, T., Schneider, M., García, O., Jones, N., Mahieu, E., Smale, D., Kotkamp, M., Robinson, J., Petropavlovskikh, I., Harris, N., Hassler, B., Hubert, D., and Tummon, F.: An update
695 on ozone profile trends for the period 2000 to 2016, Atmospheric Chemistry and Physics, 17, 10 675–10 690, https://doi.org/10.5194/acp-17-10675-2017, 2017.

Stenke, A., Schraner, M., Rozanov, E., Egorova, T., Luo, B., and Peter, T.: The SOCOL version 3.0 chemistry-climate model: Description, evaluation, and implications from an advanced transport algorithm, Geoscientific Model Development, 6, 1407–1427, https://doi.org/10.5194/gmd-6-1407-2013, 2013.

700 Studer, S., Hocke, K., Schanz, A., Schmidt, H., and Kämpfer, N.: A climatology of the diurnal variations in stratospheric and mesospheric ozone over Bern, Switzerland, Atmospheric Chemistry and Physics, 14, 5905–5919, https://doi.org/10.5194/acp-14-5905-2014, 2014.

Sukhodolov, T., Rozanov, E., Shapiro, A. I., Anet, J., Cagnazzo, C., Peter, T., and Schmutz, W.: Evaluation of the ECHAM family radiation codes performance in the representation of the solar signal, Geosci. Model Dev., 7, 1–8, https://doi.org/0.5194/gmd-7-1-2014, 2014.

Tukiainen, S., Kyrölä, E., Tamminen, J., Kujanpää, J., and Blanot, L.: GOMOS bright limb ozone data set, Atmospheric Measurement
705 Techniques, 8, 3107–3115, https://doi.org/10.5194/amt-8-3107-2015, 2015.

Vaughan, G.: Mesospheric ozone — theory and observation, Quarterly Journal of the Royal Meteorological Society, 110, 239–260, https://doi.org/10.1002/qj.49711046316, 1984.

Wang, W., Tian, W., Dhomse, S., Xie, F., Shu, J., and Austin, J.: Stratospheric ozone depletion from future nitrous oxide increases, Atmospheric Chemistry and Physics, 14, 12 967–12 982, https://doi.org/10.5194/acp-14-12967-2014, 2014.

710 Waters, J., Froidevaux, L., Harwood, R., Jarnot, R., Pickett, H., Read, W., Siegel, P., Cofield, R., Filipiak, M., Flower, D., Holden, J., Lau, G., Livesey, N., Manney, G., Pumphrey, H., Santee, M., Wu, D., Cuddy, D., Lay, R., Loo, M., Perun, V., Schwartz, M., Stek, P., Thurstans, R., Boyles, M., Chandra, K., Chavez, M., Gun-Shing Chen, Chudasama, B., Dodge, R., Fuller, R., Girard, M., Jiang, J., Yibo Jiang, Knosp, B., LaBelle, R., Lam, J., Lee, K., Miller, D., Oswald, J., Patel, N., Pukala, D., Quintero, O., Scaff, D., Van Snyder, W., Tope, M., Wagner, P., and Walch, M.: The Earth observing system microwave limb sounder (EOS MLS) on the aura Satellite, IEEE Transactions on Geoscience
715 and Remote Sensing, 44, 1075–1092, https://doi.org/10.1109/TGRS.2006.873771, 2006.

https://doi.org/10.5194/acp-2020-101
Preprint. Discussion started: 17 February 2020

Atmospheric Chemistry and Physics Discussions

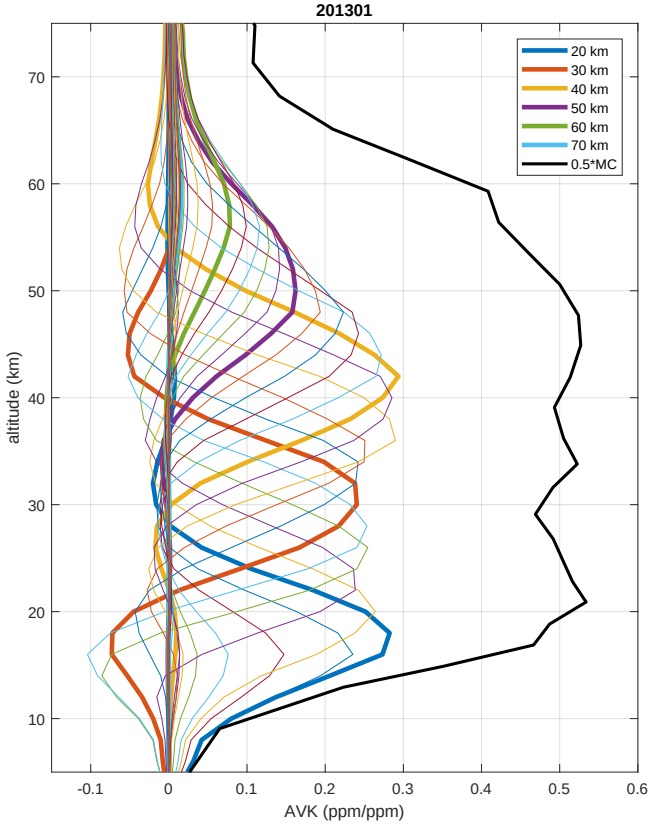

Figure 1. Example of Payerne MWR averaging kernels in ppm/ppm and measurement contribution ($\times 0.5$) for January, 2013

https://doi.org/10.5194/acp-2020-101
Preprint. Discussion started: 17 February 2020

Atmospheric Chemistry and Physics Discussions

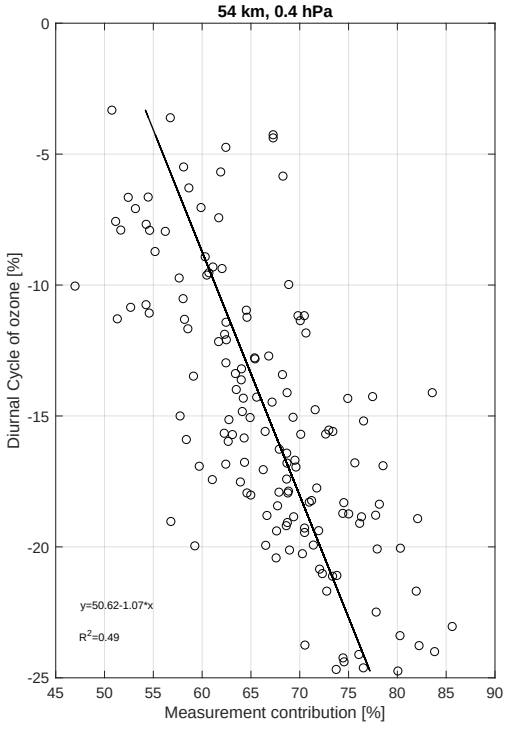

Figure 2. Ozone diurnal cycle amplitude (in % of midnight value) as a function of measurement contribution (in % of ozone content) for the lower mesosphere (0.4hPa)

https://doi.org/10.5194/acp-2020-101
Preprint. Discussion started: 17 February 2020

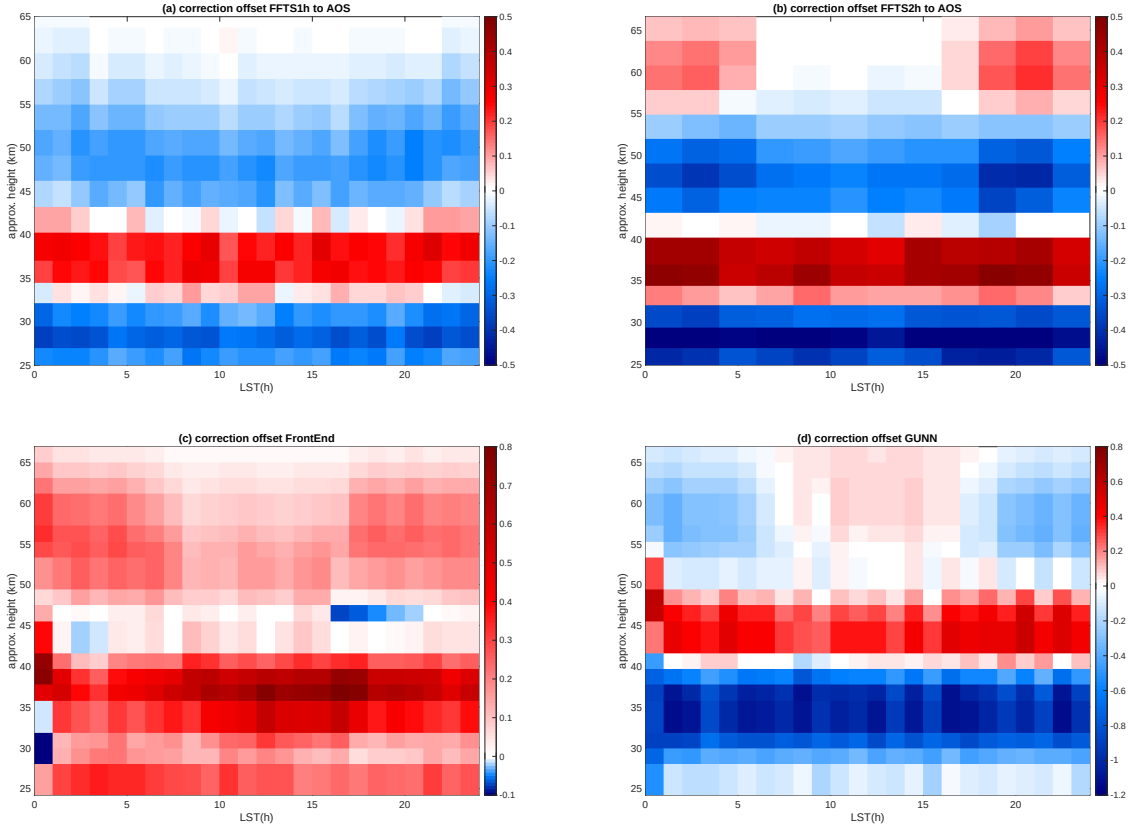

Figure 3. (a) and (b) Payerne MWR AOS setup vs FFT setup offset profiles in ppm as a function of LST, (c) correction offset for the front-end (in 2005) and (d) for the GUNN oscillator (in 2009) technical upgrades

https://doi.org/10.5194/acp-2020-101
Preprint. Discussion started: 17 February 2020

Atmospheric Chemistry and Physics Discussions

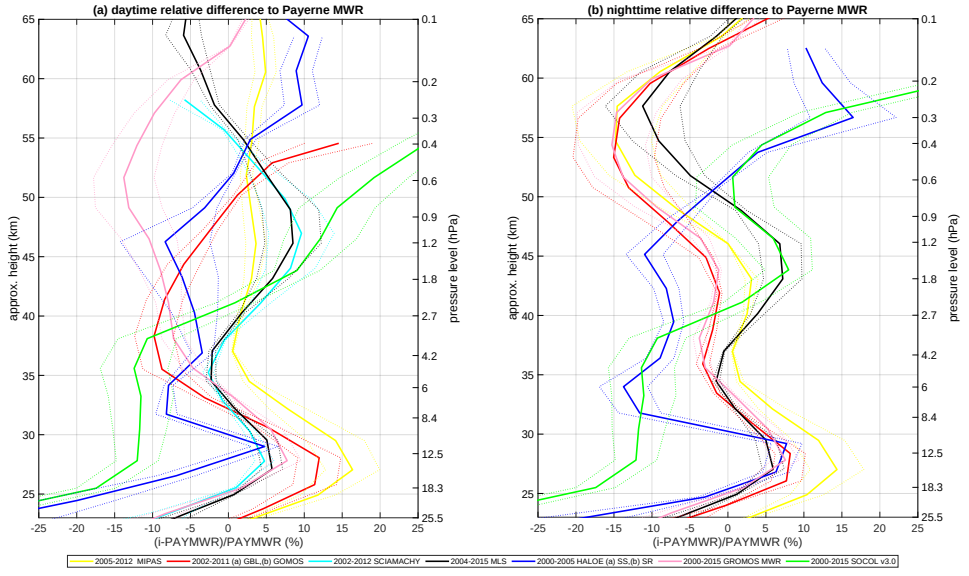

Figure 4. Payerne MWR bias vertical structure: mean of the relative difference between Payerne MWR and satellites MIPAS, MLS, GOMOS, GBL, SCIAMACHY, HALOE ((a) SS and (b) SR), and Bern MWR and SOCOL v3.0 CCM, for (a) daytime (10:00-14:00 LST) and (b) nighttime measurements (22:00-2:00 LST)

https://doi.org/10.5194/acp-2020-101
Preprint. Discussion started: 17 February 2020

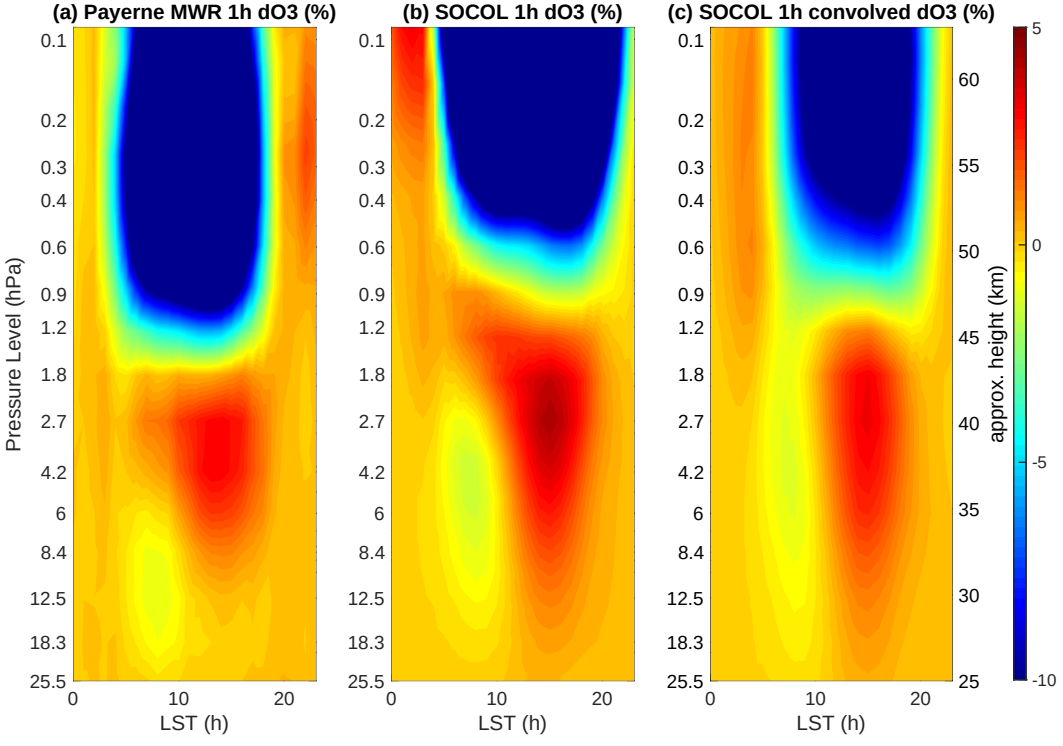

Figure 5. Annual mean O3 daily cycle measured by (a) Payerne MWR and (b)-(c) simulated by SOCOL v3.0 with a time step of 1h

https://doi.org/10.5194/acp-2020-101
Preprint. Discussion started: 17 February 2020

Atmospheric Chemistry and Physics Discussions

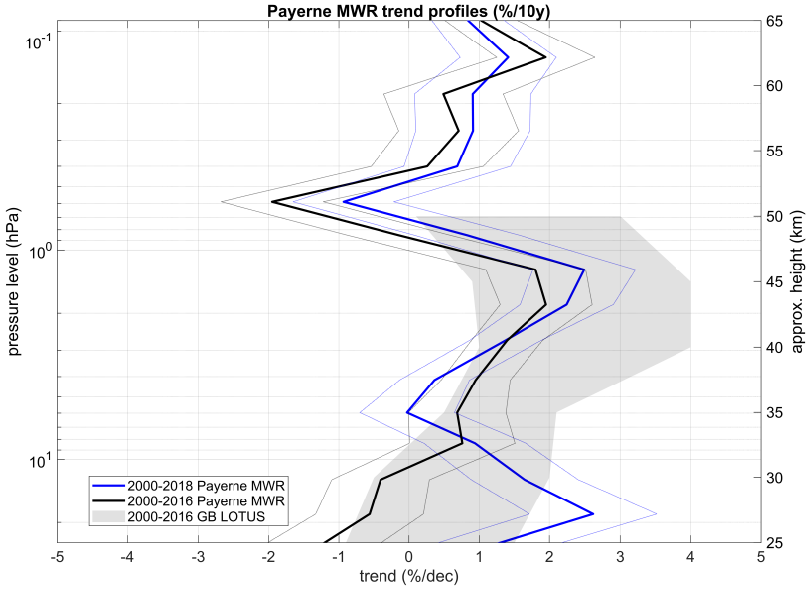

Figure 6. Payerne MWR O3 trend profiles for 2000-2016 and 2000-2018 time range, LOTUS GB 2000-2016 trend profiles

https://doi.org/10.5194/acp-2020-101
Preprint. Discussion started: 17 February 2020

Atmospheric Chemistry and Physics Discussions

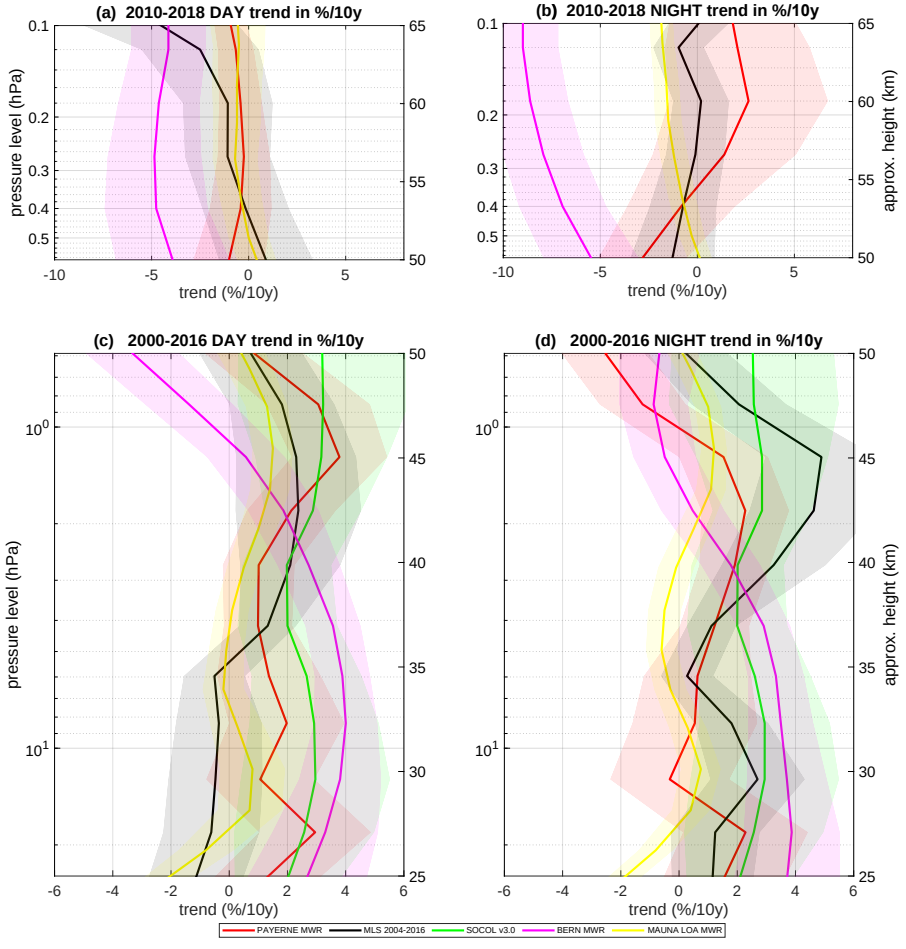

Figure 7. 2000–2018 stratospheric (c and d) and 2010–2018 low-mesospheric (a and b) day- and nighttime trend profiles for Payerne MWR, MLS, SOCOL v3.0, Bern MWR, 2000–2016 MLO MWR. The shaded areas show the 2 σ uncertainties

https://doi.org/10.5194/acp-2020-101
Preprint. Discussion started: 17 February 2020

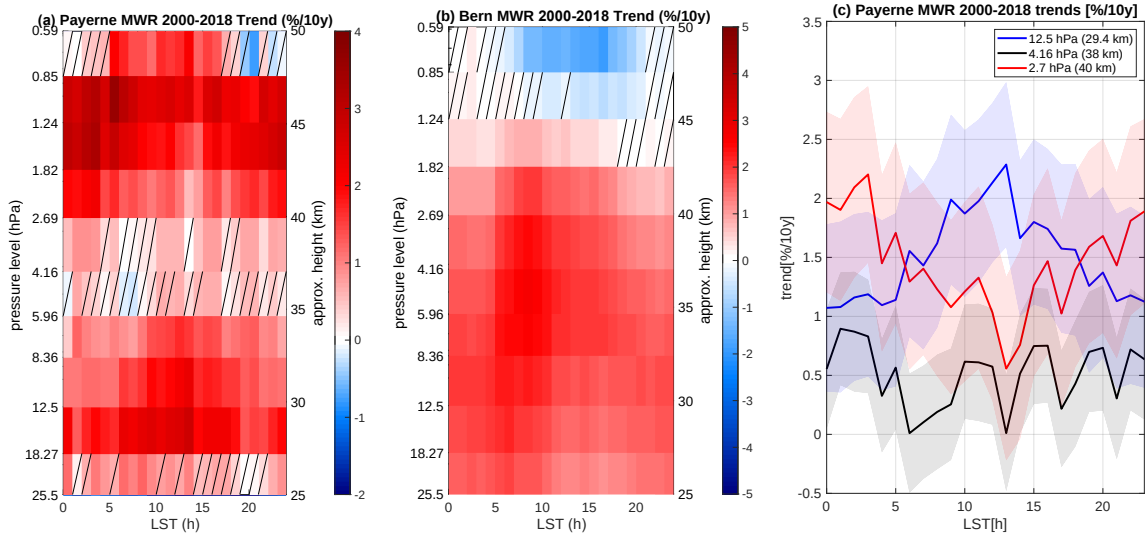

Figure 8. Long-term trends in %/dec vs LST for the 2000-2018 period. Trend estimates non significantly different from zero at 95% are hatched.(a) Payerne MWR 1h time resolution dataset (b) Bern MWR 1h time resolution dataset (c) Payerne MWR O3 trends in %/dec at 2.7 hPa (red), at morning minimum (12.5 hPa, blue) and afternoon maximum (4.16 hPa, black) pressure levels vs LST

https://doi.org/10.5194/acp-2020-101
Preprint. Discussion started: 17 February 2020

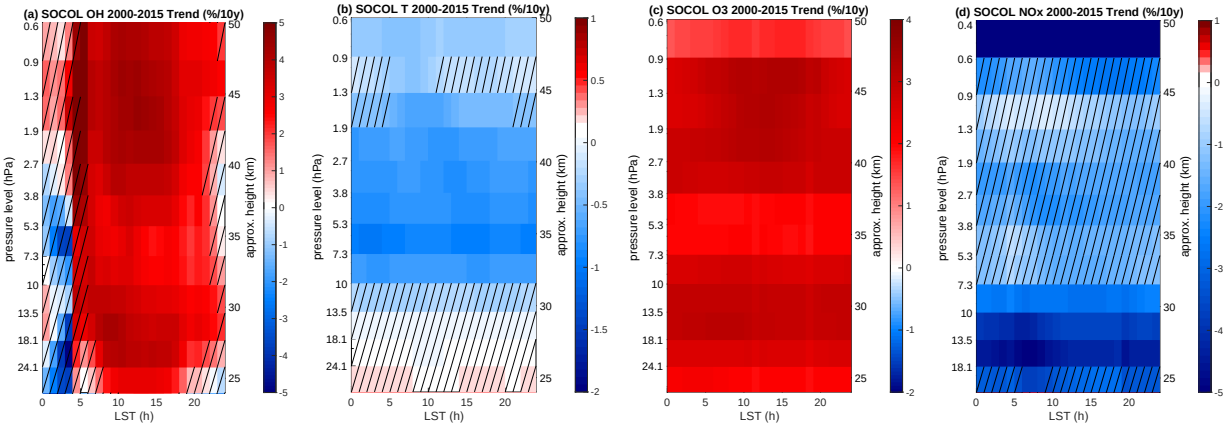

Figure 9. SOCOL v3.0 trends in %/dec vs LST (a) OH trends (b) T trends (c) O3 trends (d) NOx trends

https://doi.org/10.5194/acp-2020-101
Preprint. Discussion started: 17 February 2020

Atmospheric Chemistry and Physics Discussions

SOL	10.7 cm solar radio flux Penticton adjusted	http://www.spaceweather.gc.ca/solarflux/sx-5-mavg-eng.php
QBO10	Monthly mean zonal wind components at 10 hPa	http://www.geo.fu-berlin.de/met/ag/strat/produkte/qbo/index.html
QBO30	Monthly mean zonal wind components at 30 hPa	http://www.geo.fu-berlin.de/met/ag/strat/produkte/qbo/index.html
ENSO	Multivariate El Niño Southern Oscillation Index (MEI)	http://www.esrl.noaa.gov/psd/enso/mei/
NAO	North Atlantic Oscillations index	https://climatedataguide.ucar.edu/climate-data/hurrell-north-atlantic-oscillation-nao-index-station-based

Table 1. List of the explanatory variables used in the MLR model